

Electron spin relaxation in bulk III-V semiconductors from a fully microscopic kinetic spin Bloch equation approach

J. H. Jiang and M. W. Wu*

*Hefei National Laboratory for Physical Sciences at Microscale,
University of Science and Technology of China, Hefei, Anhui, 230026, China and*

Department of Physics, University of Science and Technology of China, Hefei, Anhui, 230026, China[†]
(Dated: February 3, 2022)

Electron spin relaxation in bulk III-V semiconductors is investigated from a fully microscopic kinetic spin Bloch equation approach where all relevant scatterings, such as, the electron–nonmagnetic-impurity, electron-phonon, electron-electron, electron-hole, and electron-hole exchange (the Bir-Aronov-Pikus mechanism) scatterings are explicitly included. The Elliot-Yafet mechanism is also fully incorporated. This approach offers a way toward thorough understanding of electron spin relaxation both near and far away from the equilibrium in the metallic regime. The dependences of the spin relaxation time on electron density, temperature, initial spin polarization, photo-excitation density, and hole density are studied thoroughly with the underlying physics analyzed. We find that these dependences are usually *qualitatively* different in the non-degenerate and degenerate regimes, whereas previous studies in the literature only focus on the non-degenerate regime. In contrast to the previous investigations in the literature, we find that: (i) In *n*-type materials, the Elliot-Yafet mechanism is *less* important than the D'yakonov-Perel' mechanism, even for the narrow band-gap semiconductors such as InSb and InAs. (ii) The density dependence of the spin relaxation time is nonmonotonic and we predict a *peak* in the metallic regime in both *n*-type and intrinsic materials. (iii) In intrinsic materials, the Bir-Aronov-Pikus mechanism is found to be negligible compared with the D'yakonov-Perel' mechanism. We also predict a peak in the temperature dependence of spin relaxation time which is due to the nonmonotonic temperature dependence of the electron-electron Coulomb scattering in intrinsic materials with small initial spin polarization. (iv) In *p*-type III-V semiconductors, the Bir-Aronov-Pikus mechanism dominates spin relaxation in the low temperature regime only when the photo-excitation density is low. When the photo-excitation density is high, the Bir-Aronov-Pikus mechanism can be comparable with the D'yakonov-Perel' mechanism only in the moderate temperature regime roughly around the Fermi temperature of electrons, whereas for higher or lower temperature it is unimportant. The relative importance of the Bir-Aronov-Pikus mechanism decreases with the photo-excitation density and eventually becomes negligible at sufficiently high photo-excitation density. The effect of electric field on spin relaxation in *n*-type III-V semiconductors is also studied with behaviors very different from those in the two-dimensional case reported. Finally, we find good agreement of our calculation with the experimental results.

PACS numbers: 72.25.Rb, 71.70.Ej, 71.10.-w, 72.20.Ht

I. INTRODUCTION

Semiconductor spintronics, which aims at utilizing or incorporating the spin degree of freedom in electronics, has attracted much interest.^{1,2,3} During the last decade, the fast developments of techniques of coherent manipulation of electron spins via optical or electrical methods^{4,5,6,7,8,9,10,11,12} have intrigued a lot of studies.³ Many of the important findings are developed in bulk GaAs or GaAs epilayers, where the spin relaxation time (SRT) was found to be as long as 130 ns,⁴ and the spin diffusion length was reported as large as 100 μm .⁵ Remarkably, it has been found that the SRT can vary by more than three orders of magnitude with temperature or electron density.⁴ The relevant spin relaxation mechanisms for electron system in the metallic regime have been recognized for a long time as: (i) the Elliot-Yafet (EY) mechanism in which electron spins have a small chance to flip during each scattering due to spin mix-

ing in the conduction band;¹³ (ii) the D'yakonov-Perel' (DP) mechanism in which the electron spins decay due to their precession around the inhomogeneous spin-orbit fields during the free flight between adjacent scattering events;¹⁴ (iii) the Bir-Aronov-Pikus (BAP) mechanism in which electrons exchange their spins with holes.¹⁵ The hyperfine interaction is another mechanism which is usually important for spin relaxation of localized electrons and ineffective in metallic regime where most of the carriers are in extended states.^{1,3,6,16,17,18}

Despite decades of study, a detailed theoretical investigation from a fully microscopic approach in bulk system has not yet been performed. Although there have been a lot of investigations on electron spin relaxation due to the three relevant mechanisms for various conditions, most of these studies use analytical expressions which are only applicable for the non-degenerate electron system, and hence make the discussion in low temperature and/or high density regime questionable.^{1,3,19} More importantly, the carrier-carrier

Coulomb scattering, which has been shown to be very important for spin relaxation in two-dimensional systems,^{20,21,22,23,24,25,26,27,28,29,30,31,32,33} has not yet been well studied in bulk system. Also, at finite spin polarization, the Coulomb Hartree-Fock (HF) term acts as an effective longitudinal magnetic field, which has been demonstrated to be able to increase the SRT by more than one order of magnitude when the initial spin polarization is high in two-dimensional electron system (2DES).^{21,34,35} However, the effect of the Coulomb HF term in bulk system has not been investigated. Another issue is that the commonly used analytical formula for spin relaxation due to the BAP mechanism is based on the elastic scattering approximation, which has been proved to be invalid for low temperature due to preemption of the Pauli blocking of electrons very recently by Zhou and Wu.²⁶ Consequently, the BAP mechanism has been demonstrated to be unimportant in two-dimensional system,²⁶ which is quite against the common belief in the literature. Whether it is still true in bulk system remains unchecked. Furthermore, in most works only the short-range electron-hole exchange interaction is considered, while the long-range part is ignored.^{1,3,19,36,37} All these questions suggest that a detailed fully microscopic investigation is needed. In this paper, we perform such a study from the fully microscopic kinetic spin Bloch equation (KSBE) approach.^{20,21,22,23,24,25,26,27,28,33,38}

Previously, the KSBE approach has been applied extensively to study spin dynamics in semiconductor nanostructures in both Markovian and non-Markovian limits and in systems both near and far away from the equilibrium (under strong static or terahertz electric field or with high spin polarization).^{20,21,22,23,24,25,26,27,28,32,33,34,38,39,40} The KSBE approach has been demonstrated to be successful in the study of spin relaxation in semiconductor quantum wells where good agreements with experiments have been achieved and many predictions have been confirmed by experiments.^{23,31,32,34,35,40,41,42,43} This approach has also been applied in the investigation of spin relaxation/dephasing in bulk GaAs many years ago by Wu and Ning, where only the electron-nonmagnetic-impurity and electron-phonon scatterings are included.⁴⁴ In this work, we include all the scatterings, especially the electron-electron Coulomb, electron-hole Coulomb, and electron-hole exchange scatterings together with the EY mechanism which are not considered in Ref. 44.

An important goal of this work is to find the dominant mechanism in different parameter regimes and for different materials from the fully microscopic KSBE approach. Previous investigations in the literature indicate that for *n*-type III-V semiconductors, the spin relaxation is mostly dominated by the DP mechanism, except at low temperature where the EY mechanism is most important; for intrinsic and *p*-type III-V semiconductors, the BAP mechanism dominates at low temperature when the hole density is high, whereas the DP mechanism dominates in other regimes.^{1,3,19,45} In the present work, from the fully

microscopic KSBE approach, however, we find that the EY mechanism is less important than the DP mechanism in *n*-type III-V semiconductors even for narrow band-gap semiconductors, such as InAs and InSb. For *p*-type III-V semiconductors, we find that the BAP mechanism dominates spin relaxation in the low temperature regime only when the photo-excitation density is low. However, when the photo-excitation density is high, the BAP mechanism can be comparable with the DP mechanism only in the moderate temperature regime roughly around the Fermi temperature of electrons, and for higher or lower temperature it is unimportant. The relative importance of the BAP mechanism decreases with the photo-excitation density and eventually becomes negligible for sufficiently high photo-excitation density. For intrinsic III-V semiconductors, the BAP mechanism is negligible.

An important method of spin injection is the hot-electron spin injection where high electric field is applied.⁴⁶ Moreover, in 2DES, the spin relaxation can be effectively manipulated by the high in-plane electric field.^{22,23,27} In this work, we also study spin relaxation in *n*-type bulk semiconductors under high electric field. We show that there is some essential difference of the electric field effect on spin dynamics between 2DES and the bulk system. Using GaAs as an example, we demonstrate that the electric field dependence of spin lifetime can be non-monotonic or monotonic depending on the lattice temperature and the densities of impurities and electrons. The underlying physics is analyzed. The results indicate that the spin lifetime can be effectively controlled by electric field.

This paper is organized as follows: In Sec. II, we introduce the KSBEs. In Sec. III, we study spin relaxation in *n*-type III-V semiconductors. In Secs. IV and V, we investigate the spin relaxation in intrinsic and *p*-type III-V semiconductors, respectively. We study the effects of electric field on spin relaxation in *n*-type III-V semiconductors in Sec. VI. Finally, we conclude in Sec. VII.

II. KSBEs

The spin dynamics is studied by solving the microscopic KSBEs derived via nonequilibrium Green function method,^{20,21,47}

$$\partial_t \hat{\rho}_{\mathbf{k}} = \partial_t \hat{\rho}_{\mathbf{k}}|_{coh} + \partial_t \hat{\rho}_{\mathbf{k}}|_{drift} + \partial_t \hat{\rho}_{\mathbf{k}}|_{scat}. \quad (1)$$

Here $\hat{\rho}_{\mathbf{k}}$ is the single particle density matrix with the diagonal terms representing the distributions of each spin band, and the off-diagonal terms denoting the correlation of the two spin bands. The coherent term is given by

$$\partial_t \hat{\rho}_{\mathbf{k}}|_{coh} = -i[\mathbf{\Omega}(\mathbf{k}) \cdot \frac{\hat{\boldsymbol{\sigma}}}{2} + \hat{\Sigma}_{HF}(\mathbf{k}), \hat{\rho}_{\mathbf{k}}]. \quad (2)$$

Here $[\ , \]$ is the commutator and $\mathbf{\Omega}(\mathbf{k}) = \mathbf{\Omega}_D(\mathbf{k}) + \mathbf{\Omega}_S(\mathbf{k})$ with

$$\mathbf{\Omega}_D(\mathbf{k}) = 2\gamma_D (k_x (k_y^2 - k_z^2), k_y (k_z^2 - k_x^2), k_z (k_x^2 - k_y^2)) \quad (3)$$

due to the Dresselhaus spin-orbit coupling (SOC)⁴⁸ and

$$\Omega_S(\mathbf{k}) = 2\beta(k_x, -k_y, 0) \quad (4)$$

due to the strain induced SOC.^{1,11,39} $\hat{\Sigma}_{\text{HF}}(\mathbf{k}) = -\sum_{\mathbf{k}'} V_{\mathbf{k}-\mathbf{k}'} \hat{\rho}_{\mathbf{k}'}$ is the Coulomb HF term of the electron-electron interaction. Previously, it was found that the Coulomb HF term serves as a longitudinal effective magnetic field which increases with the initial spin polarization. The effective magnetic field can be as large as 40 T, which blocks the inhomogeneous broadening of the \mathbf{k} -dependent spin-orbit field and reduces the spin relaxation due to the DP mechanism in 2DES.²¹ However, the effect of the HF effective magnetic field on spin relaxation in bulk system is still unknown, which is one of the goal of this paper. The drift term is given by,²²

$$\partial_t \hat{\rho}_{\mathbf{k}}|_{\text{drift}} = -e\mathbf{E} \cdot \nabla_{\mathbf{k}} \hat{\rho}_{\mathbf{k}}, \quad (5)$$

where e is the electron charge ($e < 0$) and \mathbf{E} is the electric field. As the hole spin relaxation is very fast (~ 100 fs),^{49,50} one can assume that the hole system is kept in the thermal equilibrium state where the hole distribution ($f_{\mathbf{k},m}^h$) is described by the Fermi distribution. The scattering term $\partial_t \hat{\rho}_{\mathbf{k}}|_{\text{scat}}$ contains the contri-

butions from the electron-impurity scattering $\partial_t \hat{\rho}_{\mathbf{k}}|_{ei}$, the electron-phonon scattering $\partial_t \hat{\rho}_{\mathbf{k}}|_{ep}$, the electron-electron scattering $\partial_t \hat{\rho}_{\mathbf{k}}|_{ee}$, the electron-hole Coulomb scattering $\partial_t \hat{\rho}_{\mathbf{k}}|_{eh}$, and the electron-hole exchange scattering $\partial_t \hat{\rho}_{\mathbf{k}}|_{ex}$,

$$\begin{aligned} \partial_t \hat{\rho}_{\mathbf{k}}|_{\text{scat}} = & \partial_t \hat{\rho}_{\mathbf{k}}|_{ei} + \partial_t \hat{\rho}_{\mathbf{k}}|_{ep} + \partial_t \hat{\rho}_{\mathbf{k}}|_{ee} \\ & + \partial_t \hat{\rho}_{\mathbf{k}}|_{eh} + \partial_t \hat{\rho}_{\mathbf{k}}|_{ex}. \end{aligned} \quad (6)$$

These terms read

$$\begin{aligned} \partial_t \hat{\rho}_{\mathbf{k}}|_{ei} = & -\pi \sum_{\mathbf{k}'} n_i Z_i^2 V_{\mathbf{k}-\mathbf{k}'}^2 \delta(\varepsilon_{\mathbf{k}'} - \varepsilon_{\mathbf{k}}) \left(\hat{\Lambda}_{\mathbf{k},\mathbf{k}'} \hat{\rho}_{\mathbf{k}'}^> \hat{\Lambda}_{\mathbf{k}',\mathbf{k}} \right. \\ & \times \hat{\rho}_{\mathbf{k}}^< - \hat{\Lambda}_{\mathbf{k},\mathbf{k}'} \hat{\rho}_{\mathbf{k}}^< \hat{\Lambda}_{\mathbf{k}',\mathbf{k}} \hat{\rho}_{\mathbf{k}'}^> \left. \right) + \text{H.c.}, \end{aligned} \quad (7)$$

$$\begin{aligned} \partial_t \hat{\rho}_{\mathbf{k}}|_{ep} = & -\pi \sum_{\lambda, \pm, \mathbf{k}'} |M_{\lambda, \mathbf{k}-\mathbf{k}'}|^2 \delta(\pm \omega_{\lambda, \mathbf{k}-\mathbf{k}'} + \varepsilon_{\mathbf{k}'} - \varepsilon_{\mathbf{k}}) \\ & \times \left(N_{\lambda, \mathbf{k}-\mathbf{k}'}^{\pm} \hat{\Lambda}_{\mathbf{k},\mathbf{k}'} \hat{\rho}_{\mathbf{k}'}^> \hat{\Lambda}_{\mathbf{k}',\mathbf{k}} \hat{\rho}_{\mathbf{k}}^< - N_{\lambda, \mathbf{k}-\mathbf{k}'}^{\mp} \hat{\Lambda}_{\mathbf{k},\mathbf{k}'} \right. \\ & \times \hat{\rho}_{\mathbf{k}}^< \hat{\Lambda}_{\mathbf{k}',\mathbf{k}} \hat{\rho}_{\mathbf{k}'}^> \left. \right) + \text{H.c.}, \end{aligned} \quad (8)$$

$$\begin{aligned} \partial_t \hat{\rho}_{\mathbf{k}}|_{ee} = & -\pi \sum_{\mathbf{k}', \mathbf{k}''} V_{\mathbf{k}-\mathbf{k}'}^2 \delta(\varepsilon_{\mathbf{k}'} - \varepsilon_{\mathbf{k}} + \varepsilon_{\mathbf{k}''} - \varepsilon_{\mathbf{k}''-\mathbf{k}+\mathbf{k}'}) \left[\hat{\Lambda}_{\mathbf{k},\mathbf{k}'} \hat{\rho}_{\mathbf{k}'}^> \hat{\Lambda}_{\mathbf{k}',\mathbf{k}} \hat{\rho}_{\mathbf{k}}^< \text{Tr} \left(\hat{\Lambda}_{\mathbf{k}'',\mathbf{k}''-\mathbf{k}+\mathbf{k}'} \hat{\rho}_{\mathbf{k}''-\mathbf{k}+\mathbf{k}'}^< \hat{\Lambda}_{\mathbf{k}''-\mathbf{k}+\mathbf{k}',\mathbf{k}''} \hat{\rho}_{\mathbf{k}''}^> \right) \right. \\ & \left. - \hat{\Lambda}_{\mathbf{k},\mathbf{k}'} \hat{\rho}_{\mathbf{k}}^< \hat{\Lambda}_{\mathbf{k}',\mathbf{k}} \hat{\rho}_{\mathbf{k}'}^> \text{Tr} \left(\hat{\Lambda}_{\mathbf{k}'',\mathbf{k}''-\mathbf{k}+\mathbf{k}'} \hat{\rho}_{\mathbf{k}''-\mathbf{k}+\mathbf{k}'}^> \hat{\Lambda}_{\mathbf{k}''-\mathbf{k}+\mathbf{k}',\mathbf{k}''} \hat{\rho}_{\mathbf{k}''}^< \right) \right] + \text{H.c.}, \end{aligned} \quad (9)$$

$$\begin{aligned} \partial_t \hat{\rho}_{\mathbf{k}}|_{eh} = & -\pi \sum_{\mathbf{k}', \mathbf{k}'', m, m'} V_{\mathbf{k}-\mathbf{k}'}^2 \delta(\varepsilon_{\mathbf{k}'} - \varepsilon_{\mathbf{k}} + \varepsilon_{\mathbf{k}''m}^h - \varepsilon_{\mathbf{k}''-\mathbf{k}+\mathbf{k}'m'}^h) \left[\hat{\Lambda}_{\mathbf{k},\mathbf{k}'} \hat{\rho}_{\mathbf{k}'}^> \hat{\Lambda}_{\mathbf{k}',\mathbf{k}} \hat{\rho}_{\mathbf{k}}^< |\mathcal{T}_{\mathbf{k}''-\mathbf{k}+\mathbf{k}'m'}^{\mathbf{k}''m}|^2 f_{\mathbf{k}''-\mathbf{k}+\mathbf{k}'m'}^h \right. \\ & \times (1 - f_{\mathbf{k}''m}^h) - \hat{\Lambda}_{\mathbf{k},\mathbf{k}'} \hat{\rho}_{\mathbf{k}}^< \hat{\Lambda}_{\mathbf{k}',\mathbf{k}} \hat{\rho}_{\mathbf{k}'}^> |\mathcal{T}_{\mathbf{k}''-\mathbf{k}+\mathbf{k}'m'}^{\mathbf{k}''m}|^2 (1 - f_{\mathbf{k}''-\mathbf{k}+\mathbf{k}'m'}^h) f_{\mathbf{k}''m}^h \left. \right] + \text{H.c.}, \end{aligned} \quad (10)$$

$$\begin{aligned} \partial_t \hat{\rho}_{\mathbf{k}}|_{ex} = & -\pi \sum_{\mathbf{k}', \mathbf{k}'', m, m', \chi=\pm} \delta(\varepsilon_{\mathbf{k}'} - \varepsilon_{\mathbf{k}} + \varepsilon_{\mathbf{k}''m}^h - \varepsilon_{\mathbf{k}''-\mathbf{k}+\mathbf{k}'m'}^h) \left[\hat{s}_{\chi} \hat{\rho}_{\mathbf{k}'}^> \hat{s}_{-\chi} \hat{\rho}_{\mathbf{k}}^< |\mathcal{J}_{\mathbf{k}''-\mathbf{k}+\mathbf{k}'m'}^{(\chi)\mathbf{k}''m}|^2 f_{\mathbf{k}''-\mathbf{k}+\mathbf{k}'m'}^h (1 - f_{\mathbf{k}''m}^h) \right. \\ & \left. - \hat{s}_{\chi} \hat{\rho}_{\mathbf{k}}^< \hat{s}_{-\chi} \hat{\rho}_{\mathbf{k}'}^> |\mathcal{J}_{\mathbf{k}''-\mathbf{k}+\mathbf{k}'m'}^{(\chi)\mathbf{k}''m}|^2 (1 - f_{\mathbf{k}''-\mathbf{k}+\mathbf{k}'m'}^h) f_{\mathbf{k}''m}^h \right] + \text{H.c.} \end{aligned} \quad (11)$$

In these equations, $\hat{\Lambda}_{\mathbf{k},\mathbf{k}'} = \hat{1} - i\lambda_c(\mathbf{k} \times \mathbf{k}') \cdot \hat{\sigma}$ describes the spin-mixing due to the conduction-valence band mixing which originates from the EY spin relaxation mechanism.^{1,13} Here $\lambda_c = \frac{\eta(1-\eta/2)}{3m_c E_g(1-\eta/3)}$ with $\eta = \frac{\Delta_{SO}}{\Delta_{SO} + E_g}$. E_g and Δ_{SO} are the band-gap and the spin-orbit splitting of the valence band, respectively.¹ n_i is the impurity density. Z_i is the charge number of the impurity which is taken to be $Z_i = 1$ throughout the paper. $\varepsilon_{\mathbf{k}} = k^2/2m_c$ with m_c being the conduction band effective mass. $V_{\mathbf{q}}$ is the screened Coulomb potential where

the screening is treated within the random phase approximation (RPA),^{26,51,52}

$$V_{\mathbf{q}} = \frac{V_{\mathbf{q}}^{(0)}}{1 - V_{\mathbf{q}}^{(0)} P^{(1)}(\mathbf{q})}, \quad (12)$$

where

$$P^{(1)}(\mathbf{q}) = \sum_{\mathbf{k}, \sigma} \frac{f_{\mathbf{k}+\mathbf{q}, \sigma} - f_{\mathbf{k}, \sigma}}{\varepsilon_{\mathbf{k}+\mathbf{q}} - \varepsilon_{\mathbf{k}}} + \sum_{\mathbf{k}, m, m'} |\mathcal{T}_{\mathbf{k}, m}^{\mathbf{k}+\mathbf{q}, m'}|^2 \frac{f_{\mathbf{k}+\mathbf{q}, m'}^h - f_{\mathbf{k}, m}^h}{\varepsilon_{\mathbf{k}+\mathbf{q}, m'}^h - \varepsilon_{\mathbf{k}, m}^h}. \quad (13)$$

Here $V_{\mathbf{q}}^{(0)} = e^2/(\epsilon_0 \kappa_0 q^2)$ is the bare Coulomb potential with ϵ_0 and κ_0 representing the vacuum permittivity and the static dielectric constant, respectively, $f_{\mathbf{k}, \sigma}$ is the electron distribution on σ -spin band, $f_{\mathbf{k}, m}^h$ is the hole distribution on the hole m -spin band. $\varepsilon_{\mathbf{k}, m}^h = k^2/2m_m^*$ stands for the hole energy dispersion with m_m^* being the hole effective mass. For heavy-hole ($m = \pm \frac{3}{2}$), $m_m^* = m_0/(\gamma_1 - 2\gamma_2)$; while for light-hole ($m = \pm \frac{1}{2}$), $m_m^* = m_0/(\gamma_1 + 2\gamma_2)$. Here γ_1 and γ_2 are the parameters of the Luttinger-Kohn Hamiltonian in the spherical approximation⁵² and m_0 is the free electron mass. Note that in these bands the spins are mixed.⁵² Consequently, there are form factors in the electron-hole Coulomb scattering: $|\mathcal{T}_{\mathbf{k}, m}^{\mathbf{k}+\mathbf{q}, m'}|^2 = |\langle \xi_m(\mathbf{k}) | \xi_{m'}(\mathbf{k}') \rangle|^2$ where $|\xi_m(\mathbf{k})\rangle$'s are the eigen-states of the hole Hamiltonian which can be found in Ref. 52. $M_{\lambda, \mathbf{q}}$ is the matrix element of electron-phonon interaction with λ being the phonon branch index, which is further composed of the electron-longitudinal-optical(LO)-phonon and electron-acoustic-phonon interactions. The expressions of $M_{\lambda, \mathbf{q}}$ can be found in Ref. 44. $\omega_{\lambda \mathbf{q}}$ is the phonon energy spectrum. $N_{\lambda \mathbf{q}}^{\pm} = N_{\lambda \mathbf{q}} + \frac{1}{2} \pm \frac{1}{2}$ with $N_{\lambda \mathbf{q}}$ being the phonon number at lattice temperature.

For the electron-hole exchange scattering, the form factor $|\mathcal{J}_{\mathbf{k}''-\mathbf{k}+\mathbf{k}', m}^{(\chi) \mathbf{k}'' m}|^2$ in Eq. (11) comes from the electron-hole exchange interaction. The Hamiltonian for the electron-hole exchange interaction consists of two parts: the short-range part H_{SR} and the long-range part H_{LR} .^{1,53} The short-range part contributes a term proportional to $-\frac{1}{2} \frac{\Delta E_{SR}}{|\phi_{3D}(0)|^2} \hat{\mathbf{S}} \cdot \hat{\mathbf{s}}$, where ΔE_{SR} is the exchange splitting of the exciton ground state and $|\phi_{3D}(0)|^2 = 1/(\pi a_0^3)$ with a_0 being the exciton Bohr radius. $\hat{\mathbf{S}}$ and $\hat{\mathbf{s}}$ are the hole and electron spin operators respectively. The long-range part gives a term proportional to $\frac{3}{8} \frac{\Delta E_{LT}}{|\phi_{3D}(0)|^2} (\hat{M}_1 \hat{1} + \hat{M}_z \hat{s}_z + \frac{1}{2} \hat{M}_- \hat{s}_+ + \frac{1}{2} \hat{M}_+ \hat{s}_-)$ where ΔE_{LT} is the longitudinal-transverse splitting; \hat{M}_1 , \hat{M}_z , \hat{M}_- , and $\hat{M}_+ (= \hat{M}_1^\dagger)$ are operators in hole spin space. $\hat{s}_{\pm} = \hat{s}_x \pm i\hat{s}_y$ are the electron spin ladder operators. The expressions for \hat{M} 's can be obtained from the expressions of H_{LR} in Ref. 53. Specifically, the spin-flip matrix \hat{M}_- in the spin unmixed base can be written as (in the order of $|\frac{3}{2}\rangle, |\frac{1}{2}\rangle, |-\frac{1}{2}\rangle, |-\frac{3}{2}\rangle$),

$$\hat{M}_- = \frac{1}{K^2} \begin{bmatrix} 0 & 0 & 0 & 0 \\ -\frac{2}{\sqrt{3}} K_{\parallel}^2 & \frac{4}{3} K_z K_- & \frac{2}{3} K_-^2 & 0 \\ \frac{4}{\sqrt{3}} K_z K_+ & -\frac{8}{3} K_z^2 & -\frac{4}{3} K_z K_- & 0 \\ 2K_+^2 & -\frac{4}{\sqrt{3}} K_z K_+ & -\frac{2}{\sqrt{3}} K_{\parallel}^2 & 0 \end{bmatrix}. \quad (14)$$

Here $\mathbf{K} = \mathbf{k}' + \mathbf{k}''$ is the center-of-mass momentum of the interacting electron-hole pair. $K_{\pm} = K_x \pm iK_y$ and $K_{\parallel}^2 = K_x^2 + K_y^2$. $\hat{M}_1 \hat{1} + \hat{M}_z \hat{s}_z$ corresponds to the spin-conserving process which is irrelevant in the study of spin relaxation. Summing up the contribution from the short-range and long-range parts and keeping only the spin-flip terms, one obtains

$$\mathcal{J}_{\mathbf{k}'-\mathbf{q}, m'}^{(\pm) \mathbf{k}' m} = \langle \xi_m(\mathbf{k}') | \mathcal{J}^{(\pm)} | \xi_{m'}(\mathbf{k}' - \mathbf{q}) \rangle, \quad (15)$$

with $\mathcal{J}^{(\pm)} = \left[\frac{3}{16} \frac{\Delta E_{LT}}{|\phi_{3D}(0)|^2} \hat{M}_{\pm} - \frac{1}{4} \frac{\Delta E_{SR}}{|\phi_{3D}(0)|^2} \hat{S}_{\pm} \right]$. $\hat{S}_{\pm} = \hat{S}_x \pm i\hat{S}_y$ are the hole spin ladder operators. It should be noted that in GaAs, $\Delta E_{LT} = 0.08$ meV is four times as large as $\Delta E_{SR} = 0.02$ meV.^{54,55} Thus in GaAs the long-range part of electron-hole exchange interaction should be more important than the short-range part. Later in this paper, we will compare the contributions from the short-range and long-range parts to show that the long-range part is much more important than the short-range part in GaAs. We will also compare the results from the fully microscopic KSBE approach with those from the analytical formula widely used in the literature.^{1,3,19,36,37}

In summary, all relevant spin relaxation mechanisms have been fully incorporated in our KSBE approach. By solving the KSBEs [Eq. (1)], one obtains the temporal evolution of spin density matrix $\hat{\rho}_{\mathbf{k}}$. After that, the time evolution of macroscopic quantities, such as, the electron spin density along the z -axis, $s_z(t) = \sum_{\mathbf{k}} \text{Tr}[\hat{s}_z \hat{\rho}_{\mathbf{k}}(t)]$, are obtained. By fitting the decay of s_z with an exponential decay, one obtains the SRT. The SRTs under various conditions are studied with the underlying physics discussed. The material parameters used are listed in Table I. The parameter for strain-induced SOC β is always taken to be zero unless otherwise specified. The error of our computation is less than 5% according to our test.

In the rest part of this section, we briefly comment on the merits of the fully microscopic KSBE approach. First, for the DP mechanism. Previously, the widely used analytical formula for the SRT due to the DP mechanism is^{1,3}

$$\frac{1}{\tau_{DP}} = Q \alpha^2 \frac{(k_B T)^3}{E_g} \tau_p, \quad (16)$$

where Q is a numerical constant which varies around 1 depending on the dominant momentum scattering mechanism, τ_p is the momentum relaxation time, $\alpha = 2\gamma_D \sqrt{2m_c^3 E_g}$ is a dimensionless constant. This formula is derived from

$$\tau_{DP}^{-1} = \langle (|\mathbf{\Omega}(\mathbf{k})|^2 - \Omega_z^2(\mathbf{k})) \tau_p(\mathbf{k}) \rangle \quad (17)$$

$[\tau_p(\mathbf{k})]$ is the momentum relaxation time of the state with momentum \mathbf{k} by performing ensemble averaging over the Boltzmann distribution.³ An important fact about this formula is that it is derived in the elastic scattering approximation, which artificially confines the random-walk-like spin precession due to the \mathbf{k} -dependent spin-orbit

TABLE I: Material parameters used in the calculation (from Ref. 54 unless otherwise specified)

	GaAs	GaSb	InAs	InSb
E_g (eV)	1.52	0.8113	0.414	0.2355
Δ_{SO} (eV)	0.341	0.75	0.38	0.85
m_c/m_0	0.067	0.0412	0.023	0.0136
κ_0	12.9	15.69	15.15	16.8
κ_∞	10.8	14.44	12.25	15.68
ω_{LO} (meV)	35.4	28.95	27.0	23.2
v_{sl} (10^3 m/s)	5.29	4.01	4.28	3.4081
v_{st} (10^3 m/s)	2.48	2.4	1.83	2.284
D (10^3 kg/m 3)	5.31	5.6137	5.9	5.7747
Ξ (eV)	8.5	8.3	5.8	14.0
e_{14} (V/m)	1.41×10^9	9.5×10^8	0.35×10^9	4.7×10^8
γ_D (eV·Å 3)	23.9 ^{a,b}	168 ^b	42.3 ^b	389 ^b
Δ_{ELT} (meV)	0.08 ^c	0.02 ^d	—	—
Δ_{ESR} (meV)	0.02 ^c	0.024 ^c	—	—
γ_1	6.85	11.8	19.67	35.08
γ_2	2.5 ^f	4.65 ^f	8.83 ^f	16.27 ^f

^a Ref. 56. ^b Ref. 57. ^c Ref. 55. ^d Ref. 58.

^e Ref. 45. ^f Obtained from Ref. 54 by $\frac{1}{2}(\gamma_2 + \gamma_3)$

field only within the same energy states. However, in the genuine case the inelastic electron-phonon scattering (especially the electron-LO-phonon scattering) as well as the carrier-carrier Coulomb scattering can be more important, and the random spin precession (the “inhomogeneous broadening”) should be fully counted for the whole \mathbf{k} -space, instead only within the same energy states. On the other hand, the KSBE approach, which solves the spin precession and the momentum scattering self-consistently, takes full account of the inhomogeneous broadening and the counter effects of scattering on the inhomogeneous broadening. Moreover, the electron-electron scattering (although it does not contribute to the mobility) as well as the electron-hole scattering, which have been demonstrated to have important effects on spin relaxation/dephasing in two-dimensional systems,^{20,21,22,23,24,25,26,27,28,29,30,31,32,33} are always neglected in previous studies based on Eq. (16). On the contrary, the fully microscopic KSBE approach includes both the electron-electron and electron-hole Coulomb scatterings. In this work, we will discuss the effect of the electron-electron and electron-hole Coulomb scatterings on spin relaxation.

Second, for the EY mechanism. The formula commonly used in the literature for the SRT due to the EY mechanism reads^{1,3}

$$\frac{1}{\tau_{EY}} = A \left(\frac{k_B T}{E_g} \right)^2 \eta^2 \left(\frac{1 - \eta/2}{1 - \eta/3} \right)^2 \frac{1}{\tau_p}, \quad (18)$$

where the numerical factor A is of order 1 depending on the dominant scattering mechanism. This formula, which is also based on the elastic scattering approxima-

tion, has similar problems with those of Eq. (16). On the contrary, the fully microscopic KSBE approach, which incorporates all the EY spin-flip processes in all relevant scatterings, fully takes into account of the spin relaxation due to the EY mechanism.

Third, for the BAP mechanism. The commonly used formula for the SRT due to the BAP mechanism for non-degenerate holes (assuming all holes are free) is³

$$\frac{1}{\tau_{BAP}} = \frac{2}{\tau_0} n_h a_B^3 \frac{\langle v_{\mathbf{k}} \rangle}{v_B}, \quad (19)$$

where a_B is the exciton Bohr radius, $1/\tau_0 = (3\pi/64)\Delta E_{SR}^2/E_B$ with E_B being the exciton Bohr energy, n_h is the hole density, $\langle v_{\mathbf{k}} \rangle = \langle k/m_c \rangle$ is the average electron velocity, and $v_B = 1/(m_R a_B)$ with $m_R \approx m_c$ being the reduced mass of the electron-hole pair. For degenerate holes,³

$$\frac{1}{\tau_{BAP}} = \frac{3}{\tau_0} n_h a_B^3 \frac{\langle v_{\mathbf{k}} \rangle}{v_B} \frac{k_B T}{E_{Fh}}, \quad (20)$$

with E_{Fh} denoting the Fermi energy of holes. All these formulae are obtained within the elastic scattering approximation. Previously, it has been shown that for two-dimensional system the elastic scattering approximation is invalid for low temperature regime where the Pauli blocking of electrons is important.^{26,59} In bulk system, similar problem also exists. However, the KSBE approach keeps all the electron-hole exchange scattering terms, and thus gives correct results.

Finally, we point out that for excitation far away from equilibrium, such as excitation with high spin polarization, the spin-conserving scatterings are very important for redistribution of electrons in each spin band, which also affects the spin dynamics. This effect is automatically kept in our approach, but missing in the analytical formulae.

Although the analytical formulae [Eqs. (16)-(20)] have many disadvantages, for non-degenerate electron system they still give qualitatively good results. However, quantitative analysis based on them should be questioned.

III. SPIN RELAXATION IN n -TYPE III-V SEMICONDUCTORS

A. Comparison of different spin relaxation mechanisms

In n -type III-V semiconductors, the BAP mechanism is ineffective due to the lack of holes. The remaining mechanisms are the DP and EY mechanisms. Previously, it is widely accepted in the literature that the EY mechanism dominates spin relaxation at low temperature, while the DP mechanism is important at high temperature.^{1,3,19} Most studies concerned are based on the analytical formulae [Eqs. (16) and (18)], which give

$$\frac{\tau_{EY}}{\tau_{DP}} = k_B T \tau_p^2 \frac{Q \alpha^2 E_g}{A \eta^2} \left(\frac{1 - \eta/3}{1 - \eta/2} \right)^2. \quad (21)$$

From the above equation, one arrives at the conclusion that the EY mechanism is dominant at low temperature and/or when the momentum scattering is strong (such as, for heavily doped samples). However, the electron system may enter into the degenerate regime at low temperatures and/or in heavily doped samples, in which the above conclusion fails. A revised relation is obtained by replacing $k_B T$ with the average kinetic energy $\langle \varepsilon_{\mathbf{k}} \rangle$,³

$$\frac{\tau_{\text{EY}}}{\tau_{\text{DP}}} \propto \langle \varepsilon_{\mathbf{k}} \rangle \tau_p^2 \Theta, \quad (22)$$

with $\Theta = \frac{\alpha^2 E_g}{\eta^2} \left(\frac{1-\eta/3}{1-\eta/2} \right)^2$. This is still correct only qualitatively.

TABLE II: The factor Θ for III-V semiconductors

	GaAs	GaSb	InAs	InSb	InP
Θ (eV)	0.23	0.12	3.6×10^{-4}	9.2×10^{-4}	0.27^a

^a The SOC parameter γ_D is from Ref. 57, other parameters are from Ref. 54.

In this work, we reexamine the problem from the fully microscopic KSBE approach. Let us first examine the case of InSb. InSb is a narrow band-gap semiconductor where the spin relaxation is believed to be dominated by the EY mechanism at low temperature previously.^{3,19,60} The factor Θ is much smaller than that of GaAs, which indicates the importance of the EY mechanism according to Eq. (22) (A list of the factor Θ for different materials is given in Table II). In Fig. 1(a), we plot the ratio of the SRT due to the EY mechanism τ_{EY} to that due to the DP mechanism τ_{DP} , calculated from the KSBEs, as function of temperature for various electron densities. In the calculation, $n_i \equiv n_e$. Remarkably, it is noted that the ratio $\tau_{\text{EY}}/\tau_{\text{DP}}$ is always above 1, and in most cases it is larger than 10, i.e., the spin relaxation in n -type InSb is *not* dominated by the EY mechanism. Moreover, the temperature dependence is not monotonic, which is different from the intuition given by Eq. (22). This can be understood as following: The increase of the ratio comes from the increase of $\langle \varepsilon_{\mathbf{k}} \rangle$ which is understood easily. The decrease of the ratio comes from the decrease of τ_p due to the increase of the electron-LO-phonon scattering with temperature which becomes important for $T \gtrsim 80$ K in InSb. Therefore, after a crossover regime, the ratio eventually decreases with temperature. Moreover, for large electron density $n_e \geq 10^{17} \text{ cm}^{-3}$, the electron system is in the degenerate regime and $\langle \varepsilon_{\mathbf{k}} \rangle$ changes slowly with temperature which further facilitates the decrease of the ratio. To elucidate it clearly, we plot the SRT due to the EY mechanism and DP mechanism in Fig. 1(b) and (c) respectively. It is seen from Fig. 1(b) that the SRT due to the EY mechanism always decreases with temperature due to both the increase of $\langle \varepsilon_{\mathbf{k}} \rangle$ and the enhancement of the scattering. From Fig. 1(c), it is further noted that the temperature dependence of the SRT due to the DP mechanism is, however, different

for low density and high density regimes: in low density regime, the SRT decreases with the temperature, whereas in high density regime it increases. The decreases of SRT with temperature at low density is consistent with previous studies in the literature.^{14,19} The increases of SRT with temperature at high density, however, is because that the electron-LO-phonon scattering increases with temperature faster than the inhomogeneous broadening $\sim \langle (|\mathbf{\Omega}(\mathbf{k})|^2 - \Omega_z^2(\mathbf{k})) \rangle \propto \langle \varepsilon_{\mathbf{k}}^3 \rangle$ in the degenerate regime. Note that the results for high density cases are only given at high temperatures due to the limitation of our computation power. However, according to the above analysis, the ratio in the low temperature regime should be larger than its value at 300 K for high density cases. For low density cases with temperature lower than our calculation range, both the momentum scattering and the inhomogeneous broadening change little with temperature as the electron system is degenerate. Therefore the ratio $\tau_{\text{EY}}/\tau_{\text{DP}}$ changes slowly. Consequently, it does not change the conclusion that the EY mechanism is less efficient than the DP mechanism in n -type InSb.⁶¹ In contrast, based on Eq. (22), Song and Kim reported that the EY mechanism is more important than the DP mechanism for temperature lower than 5 K.¹⁹

What makes our conclusion different from that in the literature is that most of the previous investigations use Eqs. (16) and (18) to calculate τ_{DP} and τ_{EY} .^{3,19} However, these equations are only applicable for non-degenerate electron system. If it is used in the degenerate electron system, it *exaggerates* the relative efficiency of the EY mechanism according to Eq. (21).

We further examine other two III-V semiconductors: InAs and GaAs. In Fig. 2, we plot the ratio $\tau_{\text{EY}}/\tau_{\text{DP}}$ for different electron densities as function of temperature for both InAs and GaAs. It is seen that the ratio is always larger than 1 for both InAs⁶² and GaAs, which is different from previous results in the literature.^{19,63} Especially, for GaAs the ratio is larger than 100, which indicates that the EY mechanism is *irrelevant* for n -type GaAs. The temperature dependence of the ratio is similar to that in InSb and the underlying physics is also the same.

In summary, we find that *the EY mechanism is less efficient than the DP mechanism in n -type GaAs, InAs, and InSb*. According to the data listed in Table II, we believe that the same conclusion holds for other n -type III-V semiconductors.

B. DP spin relaxation

As the BAP mechanism and the EY mechanism are unimportant for spin relaxation in n -type III-V semiconductors, in this subsection we focus on spin relaxation due to the DP mechanism. The effect of the electron-electron Coulomb scattering on spin relaxation is studied. Previously, it was found that the electron-electron scattering plays an important role in two-dimensional system.^{20,21,22,23,24,25,26,27,28} Especially, it becomes the

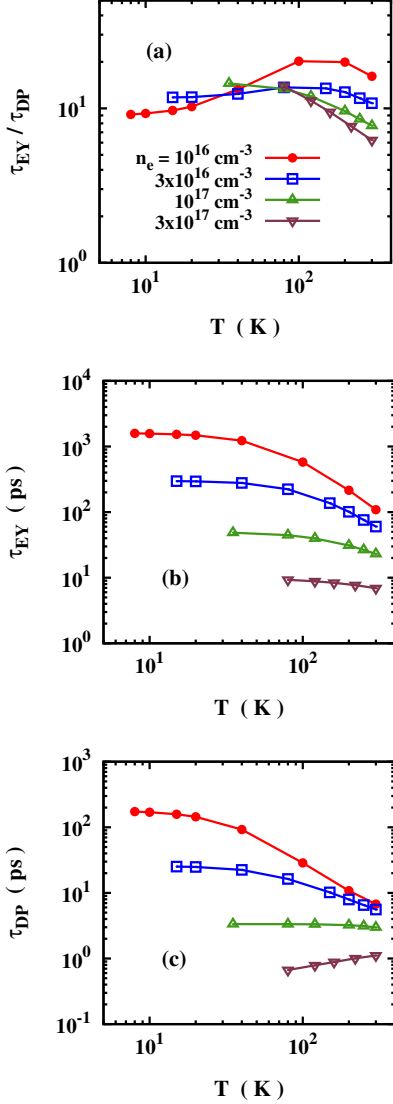


FIG. 1: (Color online) n -InSb. Ratio of the SRT due to the EY mechanism τ_{EY} to that due to the DP mechanism τ_{DP} (a), τ_{EY} (b) and τ_{DP} (c) as function of temperature for various electron densities. $n_e = 10^{16} \text{ cm}^{-3}$ (curve with \bullet), $3 \times 10^{16} \text{ cm}^{-3}$ (curve with \square), 10^{17} cm^{-3} (curve with \triangle), $3 \times 10^{17} \text{ cm}^{-3}$ (curve with ∇). The corresponding Fermi temperatures for those densities are $T_F = 144, 300, 670$, and 1390 K respectively. $n_i = n_e$.

dominant scattering mechanism in high mobility samples at low temperature, where other scattering mechanisms are relatively weak.^{25,29} Consequently $\tau_p(\mathbf{k})$ in Eq. (17) should be replaced by $\tau_p^*(\mathbf{k})$ with $1/\tau_p^*(\mathbf{k})$ including the electron-electron scattering $1/\tau_p^{ee}(\mathbf{k})$ [later we will use the symbols τ_p^* and τ_p^{ee} to denote the averaged value].^{20,21,25,29} Remarkably, the SRT due to the electron-electron scattering has *nonmonotonic* temperature dependence: in the low temperature (degenerate) regime the SRT increases with temperature as the

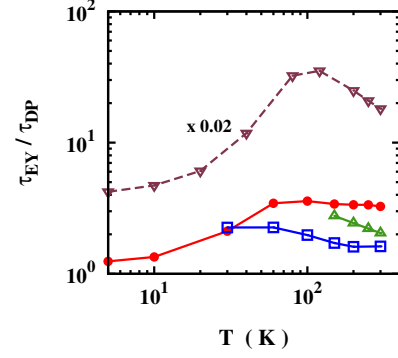


FIG. 2: (Color online) n -InAs (solid curves) and n -GaAs (dashed curve). Ratio of the SRT due to the EY mechanism τ_{EY} to that due to the DP mechanism τ_{DP} as function of temperature for various electron densities: $n_e = 10^{16} \text{ cm}^{-3}$ (curve with \bullet), $2 \times 10^{17} \text{ cm}^{-3}$ (curve with \square), 10^{18} cm^{-3} (curve with \triangle) for InAs, and $n_e = 10^{16} \text{ cm}^{-3}$ (curve with ∇) for GaAs (note that the value in the figure has been rescaled by a factor of 0.02). The Fermi temperature T_F is 85, 629, and 1840 K for InAs as well as 29 K for GaAs respectively. $n_i = n_e$.

electron-electron scattering does; in the high temperature (non-degenerate) regime the electron-electron scattering decreases with the temperature, so does the SRT.^{25,29} Thus there is a peak T_c in the temperature dependence of the SRT which is comparable with the Fermi temperature.^{25,29} This prediction was confirmed by experiments very recently.³¹ However, in bulk semiconductors, the role of electron-electron scattering in spin relaxation is still unclear. Although Glazov and Ivchenko have discussed the problem, they only gave an approximate expression of the SRT due to the electron-electron scattering in the non-degenerate regime, while the relative importance of the electron-electron scattering compared with other scattering mechanisms is not addressed.²⁹ In this subsection, we present a close study on the effect of the electron-electron scattering on spin relaxation in bulk semiconductors.

1. Electron density dependence of SRT

We first discuss the electron density dependence of the SRT. It is noted that during the variation of electron density, the impurity density also varies as $n_i = n_e$. This is different from the situation in 2DES, where the impurity density can be different from the electron density. In Fig. 3(a), we plot the SRT as function of electron density for $T = 40 \text{ K}$. It is noted that, remarkably, the density dependence of the SRT is *nonmonotonic* and there is a peak in the $\tau-n_e$ curve. Previously, the nonmonotonic density dependence of the SRT was observed in low temperature ($T \leq 5 \text{ K}$) measurements, where the localized electrons play an important role and the electron system is in the Mott metal-insulator transition area.^{4,6,16,17} The

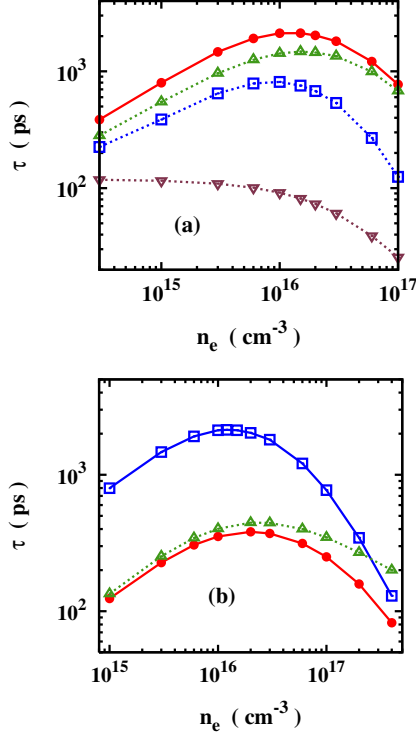


FIG. 3: (Color online) n -GaAs at $T = 40$ K. (a) SRT τ as function of electron density n_e ($n_i = n_e$) from full calculation (curve with \bullet), from calculation with only the electron-electron scattering (curve with \square), with only the electron-impurity scattering (curve with \triangle), and with only the electron-phonon scattering (curve with ∇); (b) SRT τ as function of electron density n_e ($n_i = n_e$) for the case with strain (curve with \bullet : with both the linear and the cubic SOC; curve with \triangle : with only the linear SOC) and the case without strain (curve with \square).

localized electrons have different spin relaxation mechanisms and the scattering between the localized electrons and free electrons gives rise to the nonmonotonic density dependence.^{16,17} It is noted that, up till now, there is no report on the nonmonotonic density dependence in the metallic regime in n -type bulk III-V semiconductors. It should be further pointed out that the nonmonotonic density dependence and the appearance of the peak is a universal behavior in the metallic regime in n -type bulk III-V semiconductors.

We also plot the SRTs calculated with only the electron-electron scattering (curve with \square), with only the electron-impurity scattering (curve with \triangle), and with only the electron-phonon scattering (curve with ∇) in the figure to elucidate the role of these scatterings in spin dynamics. It is noted that the electron-impurity and electron-electron scatterings are the relevant scattering mechanisms, while the electron-phonon scattering is much weaker than the two as the temperature is low. Interestingly, both the electron-electron scattering and the electron-impurity scattering lead to nonmonotonic den-

sity dependence of SRT.

For the SRT due to the electron-electron scattering, the nonmonotonic behavior comes from the nonmonotonic density dependence of the electron-electron scattering. The density and temperature dependences of the electron-electron scattering have been investigated in spin-unrelated problems.⁶⁴ From these works, after some approximation, the asymptotic density and temperature dependences of the electron-electron scattering time τ_p^{ee} in the degenerate and non-degenerate regimes are given by,^{29,64}

$$\tau_p^{ee} \propto n_e^{2/3}/T^2 \quad \text{for } T \ll T_F, \quad (23)$$

$$\tau_p^{ee} \propto T^{3/2}/n_e \quad \text{for } T \gg T_F. \quad (24)$$

From above equations, one notices that the electron-electron scattering in the non-degenerate and degenerate regimes has different density and temperature dependence. In the non-degenerate (low density) regime the electron-electron scattering increases with electron density, while the inhomogeneous broadening $\sim \langle (|\mathbf{\Omega}(\mathbf{k})|^2 - \Omega_z^2(\mathbf{k})) \rangle$ changes slowly as the distribution function is close to the Boltzmann distribution. The SRT thus increases with density. In degenerate (high density) regime, both τ_p^{ee} and the inhomogeneous broadening increases with electron density. Thus, the SRT, which can be estimated as $\tau \sim 1/[\langle |\mathbf{\Omega}(\mathbf{k})|^2 - \Omega_z^2(\mathbf{k}) \rangle \tau_p^{ee}]$,^{25,29} decreases with density.

For the SRT due to the electron-impurity scattering, the scenario is similar: In the non-degenerate regime, the distribution function is close to the Boltzmann distribution. The inhomogeneous broadening hence changes slowly with density. The electron-impurity scattering increases as $\propto n_i \langle V_q^2 \rangle$, which increases with the impurity density because $\langle V_q^2 \rangle$ changes little with the density when the distribution is close to the Boltzmann distribution. The SRT hence increases with density. In the degenerate regime, the inhomogeneous broadening increases as $\sim \langle (|\mathbf{\Omega}(\mathbf{k})|^2 - \Omega_z^2(\mathbf{k})) \rangle \propto k_F^6 \propto n_e^2$. On the other hand, the electron-impurity scattering decreases with density because it is proportional to $\sim n_i V_{k_F}^2 \propto n_e/k_F^4 \propto n_e^{-1/3}$. Consequently, the SRT decreases with density.

Therefore, both the electron-electron and electron-impurity scatterings contribute to the nonmonotonic density dependence of the SRT. The peak density n_c appears in the crossover regime, where the corresponding Fermi temperature is comparable with the lattice temperature. A careful calculation gives the peak density as $n_c = 1.4 \times 10^{16} \text{ cm}^{-3}$, with the corresponding Fermi temperature being 37 K, close to the lattice temperature of 40 K.

We further discuss the electron density dependence of the SRT with strain-induced SOC. In Fig. 3(b), we plot the density dependence of the SRT for $T = 40$ K under strain with $n_i = n_e$. We choose $\beta = 2.6 \text{ meV}\cdot\text{\AA}$.¹¹ For this value, the SOC is dominated by the linear term due to strain at low density. However, in high density regime ($n_e > 2 \times 10^{17} \text{ cm}^{-3}$), the cubic Dressel-

haus term can surpass the linear term. It is noted that the density dependence is also nonmonotonic and exhibits a peak. The underlying physics is similar: In the non-degenerate regime, the SRT increases with the density because both electron-electron and electron-impurity scattering increase with density and the inhomogeneous broadening changes little. In the degenerate regime, the inhomogeneous broadening increases as $\propto k_F^2 \propto n_e^{2/3}$, whereas both the electron-electron and electron-impurity scatterings decrease with the electron density, which thus leads to the decrease of the SRT with density. It is further noted that the peak is at $n_c = 2 \times 10^{16} \text{ cm}^{-3}$ which is larger than the peak density in the case without strain. This is because that the inhomogeneous broadening increases as $\langle k^2 \rangle$, which is much slower than that of $\langle k^6 \rangle$ in the strain-free case. Nevertheless, the increase of the scattering with density remains the same, therefore the peak shows up at a larger electron density. This is also confirmed in the figure that the SRT with only the linear term decreases slower than the one with only the cubic Dresselhaus term in the high density regime. However, in the low density regime, the SRT in the case with strain increases as fast as the one in the strain-free case. This is because here the increase of the SRT is due to the increase of the scattering, whereas the inhomogeneous broadening changes little.

2. Temperature dependence of SRT

We now study the temperature dependence of the SRT. In Fig. 4, the SRT as function of temperature is plotted for $n_e = 10^{17} \text{ cm}^{-3}$. From the figure, it is seen that the SRT decreases with temperature monotonically, which coincides with previous experimental results.^{4,65,66,67} The trend is also the same as that in the 2DES with high impurity density.²⁵ However, for high mobility 2DES, which can be achieved by modulation doping, the temperature dependence of the SRT is nonmonotonic and there is a peak T_c around the Fermi temperature due to the electron-electron scattering.²⁵ In bulk n -type materials as the impurity density is always equal to or larger than the electron density, this peak disappears. Nevertheless, similar effect can be obtained if one artificially reduces the impurity density. For example when $n_i = 0.01n_e$, it is seen from Fig. 4 that the SRT shows nonmonotonic behavior with a peak around 40 K.

3. Dependence of initial spin polarization on spin relaxation: the effect of the Coulomb HF term

We now turn to the dependence of initial spin polarization on spin relaxation. Previously, it was found that at finite spin polarization, the Coulomb HF term serves as an effective magnetic field along the direction of the spin polarization.²¹ The effective magnetic field can be

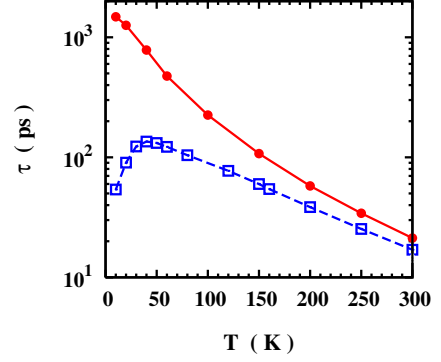


FIG. 4: (Color online) n -GaAs. SRT τ as function of T for $n_i = n_e$ (solid curve with \bullet) and $n_i = 0.01n_e$ (dashed curve with \square). $n_e = 10^{17} \text{ cm}^{-3}$.

as large as 40 T at high spin polarization in 2DES which suppresses the DP spin relaxation.²¹ This effect was first predicted by Weng and Wu²¹ and then confirmed by experiments very recently.^{34,35,42} However, the effect of the Coulomb HF term on spin relaxation in bulk system still needs to be evaluated. Here, we present such an investigation.

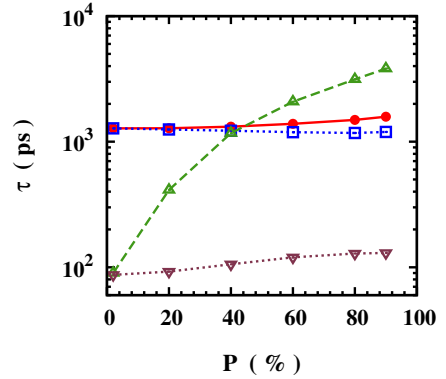


FIG. 5: (Color online) n -GaAs. Dependence of SRT τ on initial spin polarization P for $n_i = n_e$ with (without) the Coulomb HF term [curve with \bullet (\square)] and for $n_i = 0.01n_e$ with (without) the Coulomb HF term [curve with \triangle (∇)]. $n_e = 10^{17} \text{ cm}^{-3}$ and $T = 20 \text{ K}$.

The Coulomb HF term for spin polarization along, e.g., the z -direction can be written as

$$\hat{\Sigma}_{\text{HF}}(\mathbf{k}) = - \sum_{\mathbf{k}'} V_{\mathbf{k}-\mathbf{k}'} (f_{\mathbf{k}'\uparrow} - f_{\mathbf{k}'\downarrow}) \hat{s}_z. \quad (25)$$

The corresponding effective magnetic field is along the z -axis,

$$B_{\text{HF}}(\mathbf{k}) = - \sum_{\mathbf{k}'} V_{\mathbf{k}-\mathbf{k}'} (f_{\mathbf{k}'\uparrow} - f_{\mathbf{k}'\downarrow}) / g\mu_B. \quad (26)$$

Under this effective magnetic field, the spin precession is blocked and the SRT is elongated.^{21,29} Recently, this effective magnetic field has been probed

experimentally,^{35,42} and its effect on spin accumulation in 2DES is also discussed theoretically.⁶⁸

In Fig. 5, we plot the SRT as function of the initial spin polarization P for $n_e = 10^{17} \text{ cm}^{-3}$ and $T = 20 \text{ K}$. It is seen that the SRT increases with the initial spin polarization. To elucidate the effect of the Coulomb HF term, we also plot the results from the calculation without the Coulomb HF term. The results indicate that the increase of the SRT is due to the Coulomb HF term. However, the increment is less than 50%. Previously, it was shown in 2DES that the SRT can increase over 30 times for low impurity case at 120 K, while less than 3 times for high impurity or high temperature case where the scattering is strong.²¹ The results can be understood as follows: The SRT under the HF effective magnetic field can be estimated as¹ $\tau_s(P) = \tau_s(P=0)[1 + (g\mu_B B_{HF}\tau_p^*)^2]$ where B_{HF} is the averaged effective magnetic field. Thus the effect of the HF effective magnetic field increases with τ_p^* , i.e., the effect is more pronounced for weak scattering case, such as the low impurity density case. However, in bulk system the impurity density is always equal to or larger than the electron density $n_i \geq n_e$, therefore the effect of the Coulomb HF term is suppressed. This can be seen from the calculation with $n_i = 0.01n_e$ (the artificial case). The results are also plotted in the figure. One finds that the Coulomb HF term effectively enhances the SRT at low impurity density by 40 times. Therefore, due to the large impurity density ($n_i \geq n_e$), the SRT is insensitive to the initial spin polarization in n -type bulk III-V semiconductors. We have checked that the conclusion holds for other cases with different temperatures, electron densities and materials.

IV. SPIN RELAXATION IN INTRINSIC III-V SEMICONDUCTORS

In this section we study spin relaxation in intrinsic III-V semiconductors. For intrinsic semiconductors, the electrons and holes are created by optical excitation, and their numbers are equal. Compared to n -type semiconductors, there are two new scattering mechanisms: the electron-hole Coulomb and electron-hole exchange scatterings, where the latter corresponds to the BAP mechanism. Another important property of intrinsic semiconductors is that the impurity density is very low (we take $n_i = 0$), which offers a good platform for demonstrating the effect of the many-body carrier-carrier scattering on spin relaxation. Moreover, the effect of the Coulomb HF term would be enhanced as the electron-impurity scattering can be eliminated. Our first goal is to compare the relative efficiency of the DP mechanism and the BAP mechanism. After that we also study the temperature and photo-excitation density N_{ex} dependence of the SRT. The role of electron-hole Coulomb scattering as well as the effect of the Coulomb HF term are also addressed. We further compare the results from the KSBEs with those from the widely used analytical formulae [Eqs. (19) and

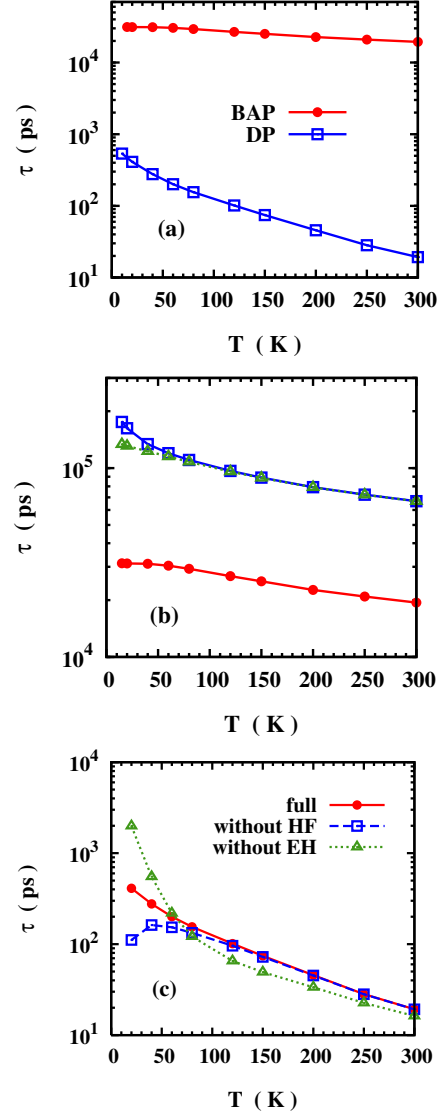


FIG. 6: (Color online) Intrinsic GaAs with $N_{ex} = 10^{17} \text{ cm}^{-3}$. (a) SRT τ due to the BAP and DP mechanisms as function of temperature. (b) SRT due to the BAP mechanism calculated from Eq. (19) (dotted curve with \triangle), from the KSBE approach with both long-range and short-range exchange scatterings (solid curve with \bullet) as well as from the KSBE approach with only the short-range exchange scattering (solid curve with \square). (c) SRT due to the DP mechanism from full calculation (solid curve with \bullet), from the calculation without the Coulomb HF term (dashed curve with \square), and from the calculation without the electron-hole Coulomb scattering (dotted curve with \triangle). For electrons $T_F = 136 \text{ K}$, and for holes $T_F = 16 \text{ K}$.

(20)]. The initial spin polarization is chosen to be 50% which corresponds to circularly polarized optical excitation. We focus on GaAs, while the situation is similar for other III-V semiconductors.⁶⁹

In Fig. 6(a), we plot the SRTs due to the DP and BAP mechanisms as function of temperature for $N_{ex} =$

10^{17} cm^{-3} . The SRT due to the BAP mechanism alone is calculated by removing the spin precession due to the SOC, but keeping all the scattering terms. It is noted that the SRT due to the BAP mechanism is larger than that due to the DP mechanism by more than one order of magnitude, which indicates that the BAP mechanism is negligible for intrinsic GaAs.⁷⁰ Moreover, the spin relaxation due to the DP mechanism increases with temperature more rapidly than that due to the BAP mechanism at high temperature. This is because the increase of spin relaxation due to the DP mechanism mainly comes from the increase of the inhomogeneous broadening which is proportional to T^3 in high temperature (non-degenerate) regime. Meanwhile, according to Eq. (19), the increase of spin relaxation due to the BAP mechanism mainly comes from the increase of $\langle v_k \rangle$ which is proportional to $T^{0.5}$ in that regime.

For a close examination of the BAP mechanism, we also plot the SRT limited by the short-range electron-hole exchange scattering calculated from the KSBEs in Fig. 6(b). It is seen that the SRT limited by the short-range electron-hole exchange scattering is much larger than that limited by both long- and short-range exchange scattering. This confirms that the long-range scattering is more important than the short-range one in GaAs as ΔE_{LT} is four times larger than ΔE_{SR} . Therefore, previous investigations^{3,19,36} with only the short-range exchange scattering included are questionable. Moreover, to check the validity of the widely used elastic scattering approximation, we also compare the results from the KSBEs with those from the elastic scattering approximation. Under the elastic scattering approximation,¹

$$\frac{1}{\tau_{\text{BAP}}(\mathbf{k})} = 4\pi \sum_{\mathbf{q}, \mathbf{k}', m, m'} \delta(\varepsilon_{\mathbf{k}} + \varepsilon_{\mathbf{k}'}^{h, m'} - \varepsilon_{\mathbf{k}-\mathbf{q}} - \varepsilon_{\mathbf{k}'+\mathbf{q}}^h) \times |\mathcal{J}_{\mathbf{k}'m'}^{(-) \mathbf{k}'+\mathbf{q}m}|^2 f_{\mathbf{k}'m'}^h (1 - f_{\mathbf{k}'+\mathbf{q}m}^h). \quad (27)$$

The SRT is then obtained by averaging over the electron distribution. Eqs. (19) and (20) are derived from the above equation under some approximations. For example, by including only the short-range exchange scattering and ignoring the light-hole contribution as well as the term of $(1 - f_{\mathbf{k}'+\mathbf{q}m}^h)$, Eq. (19) is obtained. To show that the elastic scattering approximation fails in the degenerate regime, we compare our results with the results from Eq. (27). For simplicity, we include only the short-range exchange scattering. In Fig. 6(b), we plot the SRT obtained from Eq. (27) as the dotted curve. It is seen that the result from Eq. (27) agrees well with our result from the KSBEs at high temperature, but deviates at low temperature. The deviation is due to the Pauli blocking of electrons in the degenerate regime, which is neglected in the elastic scattering approximation ($T_F = 136 \text{ K}$).⁷¹

We also discuss the effect of the electron-hole Coulomb scattering and the Coulomb HF term on spin relaxation due to the DP mechanism. In Fig. 6(c), we plot the SRTs due to the DP mechanism obtained from the full calculation, from the calculation without the electron-hole

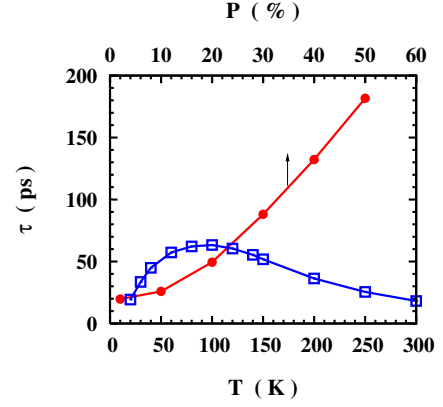


FIG. 7: (Color online) Intrinsic GaAs with $N_{ex} = 2 \times 10^{17} \text{ cm}^{-3}$. SRT τ as function of temperature for $P = 2\%$ (curve with \square) and the SRT as function of initial spin polarization P for $T = 20 \text{ K}$ (curve with \bullet) (note that the scale of P is on the top of the frame).

Coulomb scattering, and from the calculation without the Coulomb HF term.

Let us first examine the effect of the Coulomb HF term on spin relaxation. It is seen that the Coulomb HF term has important effect on spin relaxation only for low temperature case⁷² ($T < 60 \text{ K}$) which is consistent with the results in 2DES.²¹

Let us now turn to the effect of the electron-hole Coulomb scattering. It is seen that without the electron-hole Coulomb scattering the SRT is larger for $T < 60 \text{ K}$ but smaller for $T > 60 \text{ K}$ compared with that from the full calculation. This behavior can be understood as following: For $T < 60 \text{ K}$, the Coulomb HF term has important effect on spin relaxation. The HF effective magnetic field elongates the SRT. According to the analysis in Sec. III B3, this effect increases with the momentum scattering time. Without the electron-hole Coulomb scattering the momentum scattering time is elongated, which enhances the effect and leads to longer SRT. For higher temperature ($T > 60 \text{ K}$), the effect of the Coulomb HF term is weak,⁷² and the system returns back to the motional narrowing regime. The SRT thus decreases when the electron-hole Coulomb scattering is removed. The results indicate that the electron-hole Coulomb scattering is comparable with the electron-electron and electron-LO-phonon scatterings. In other words, besides the screening from holes, the main contribution of the hole system to electron spin relaxation comes from the electron-hole Coulomb scattering in intrinsic semiconductors.

In Fig. 7, we plot the SRT as function of temperature for $N_{ex} = 2 \times 10^{17} \text{ cm}^{-3}$ with $P = 2\%$. In Sec. III B2, we showed that there is a peak in the temperature dependence of SRT due to the electron-electron Coulomb scattering when the impurity density is low. In intrinsic semiconductors, as the impurity density is very low, the peak may appear. Indeed, we find that the SRT has a

peak at $T_c \sim 100$ K. The peak temperature T_c is comparable with the Fermi temperature ($T_F = 216$ K) [Actually, our calculation indicates that the peak temperature T_c is around $T_F/3$ and lies in the range of $(T_F/4, T_F/2)$ depending on the carrier density.] Nevertheless, at high spin polarization, such as $P = 50\%$, the peak disappears as indicated in Fig. 6(c). This peak can be observed within current technology of optical orientation. However, up till now, no such experimental investigation has been performed. In Fig. 7, we also plot the SRT as function of initial spin polarization at $T = 20$ K. It is seen that the SRT is elongated by 9 times when P is tuned from 2% to 50%. Therefore, the effect of the Coulomb HF term can also be observed in intrinsic materials and is more pronounced compared to the n -type case.

We further plot the density dependence of the SRT in Fig. 8 for both low temperature ($T = 40$ K) and room temperature ($T = 300$ K) cases. It is seen that for both cases the BAP mechanism is far less efficient than the DP mechanism. Another remarkable feature is that the SRT shows a *nonmonotonic* photo-excitation density dependence with a peak at some density n_c which resembles that in n -type materials. Further calculation gives $n_c = 0.8 \times 10^{16} \text{ cm}^{-3}$ ($T_F = 25$ K) for $T = 40$ K case and $n_c = 0.9 \times 10^{17} \text{ cm}^{-3}$ ($T_F = 127$ K) for $T = 300$ K case. Interestingly, two recent experiments give different photo-excitation density dependence of SRT at room temperature: in Ref. 32 the SRT decreases with N_{ex} where $N_{ex} > 10^{17} \text{ cm}^{-3}$, while in Ref. 73 the SRT increases with N_{ex} where the photo-excitation density is lower. These observations are consistent with our results. However, the peak is not observed in these works.

We then discuss the effects of the electron-hole Coulomb scattering and the Coulomb HF term on the spin relaxation for $T = 40$ K as function of photo-excitation density. In Fig. 8(c), we plot the SRTs obtained from the full calculation, from the calculation without the electron-hole Coulomb scattering, and from the calculation without the Coulomb HF term. It is seen that the Coulomb HF term plays a visible role only for high densities, as the HF effective magnetic field increases with electron density.⁷² Similar to the temperature dependence [Fig. 6(c)], without the electron-hole Coulomb scattering, the SRT is larger for $N_{ex} > 3 \times 10^{16} \text{ cm}^{-3}$ where the Coulomb HF term plays a prominent role, while it is smaller for lower photo-excitation densities where the Coulomb HF term is unimportant. Notably, the peak of SRT still exists when the Coulomb HF term is removed, which implies that the degree of initial spin polarization is irrelevant for the existence of the peak.

V. ELECTRON SPIN RELAXATION IN p -TYPE III-V SEMICONDUCTORS

In this section, we study spin relaxation in p -type III-V semiconductors. The main sources of spin relaxation have been recognized as the BAP mechanism and the DP

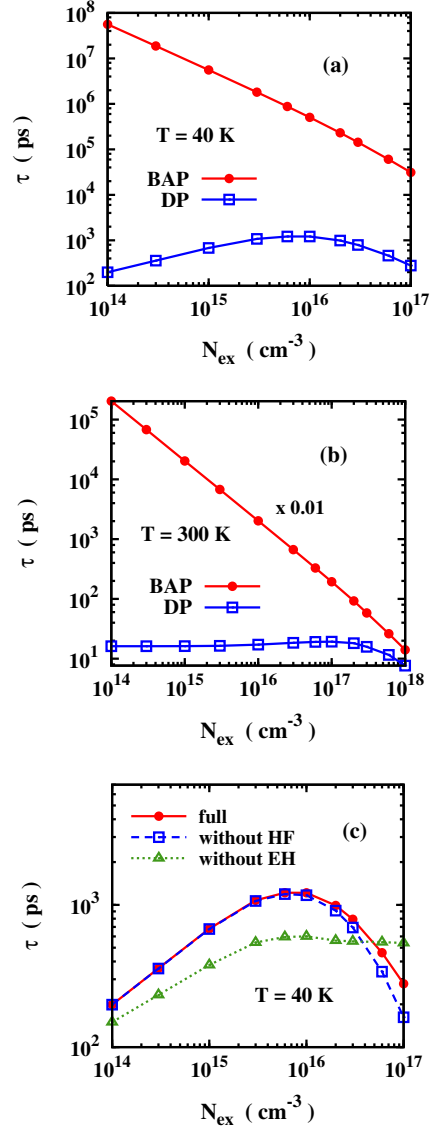


FIG. 8: (Color online) Intrinsic GaAs. SRT τ due to the BAP mechanism and that due to the DP mechanism as function of photo-excitation density N_{ex} at: $T = 40$ K (a) and $T = 300$ K (b) (note that the value of τ_{BAP} in figure (b) has been rescaled by a factor of 0.01). (c): the SRT due to the DP mechanism from the full calculation (curve with \bullet), from the calculation without the Coulomb HF term (curve with \square), and from the calculation without the electron-hole Coulomb scattering (curve with \triangle) for $T = 40$ K.

mechanism.⁷⁴ We first compare the relative efficiency of the two mechanisms for various hole densities and temperatures. After that, the hole density and the photo-excitation density dependences of the SRT at given temperature are also discussed.

We first address the relative importance of the BAP and DP mechanisms for various hole densities and temperatures in GaAs. The electrons are created by photo-excitation with $P = 50\%$ (i.e., we assume ideal optical orientation by circularly polarized light). In order to

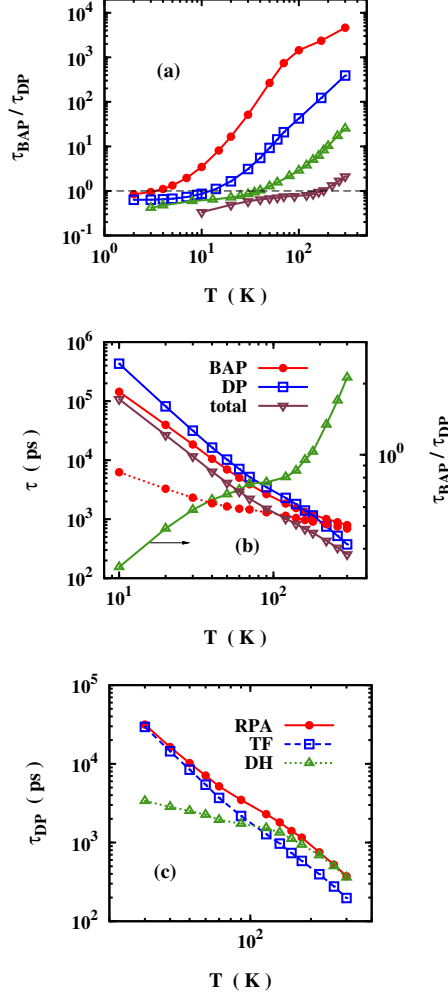


FIG. 9: (Color online) *p*-GaAs. Ratio of the SRT due to the BAP mechanism to that due to the DP mechanism as function of temperature for various hole densities with $N_{ex} = 10^{14} \text{ cm}^{-3}$ and $n_i = n_h$. (a): $n_h = 3 \times 10^{15} \text{ cm}^{-3}$ (curve with \bullet), $3 \times 10^{16} \text{ cm}^{-3}$ (curve with \square), $3 \times 10^{17} \text{ cm}^{-3}$ (curve with \triangle), and $3 \times 10^{18} \text{ cm}^{-3}$ (curve with ∇). The hole Fermi temperatures for these densities are $T_{Fh} = 1.6, 7.3, 34,$ and 156 K , respectively. The electron Fermi temperature is $T_F = 1.4 \text{ K}$. (b): The SRTs due to the BAP and DP mechanisms, the total SRT, together with the ratio $\tau_{\text{BAP}}/\tau_{\text{DP}}$ (curve with \triangle) versus the temperature for $n_h = 3 \times 10^{18} \text{ cm}^{-3}$. The dotted curve represents the SRT due to the BAP mechanism without the Pauli blocking of holes. Note the scale of $\tau_{\text{BAP}}/\tau_{\text{DP}}$ is on the right hand side of the frame. (c): The SRTs due to the DP mechanism with the TF (curve with \square), DH (curve with \triangle), and the RPA (curve with \bullet) screenings.

avoid exaggerating the DP mechanism, we use the SOC parameter fitted from the experimental data in Ref. 4, i.e., $\gamma_D = 8.2 \text{ eV} \cdot \text{\AA}^3$ (see Appendix A) throughout this section, which is smaller than the value from the $\mathbf{k} \cdot \mathbf{p}$ theory $\gamma_D = 23.9 \text{ eV} \cdot \text{\AA}^3$.^{56,57}

We first concentrate on low photo-excitation density regime, where we choose $N_{ex} = 10^{14} \text{ cm}^{-3}$. The ra-

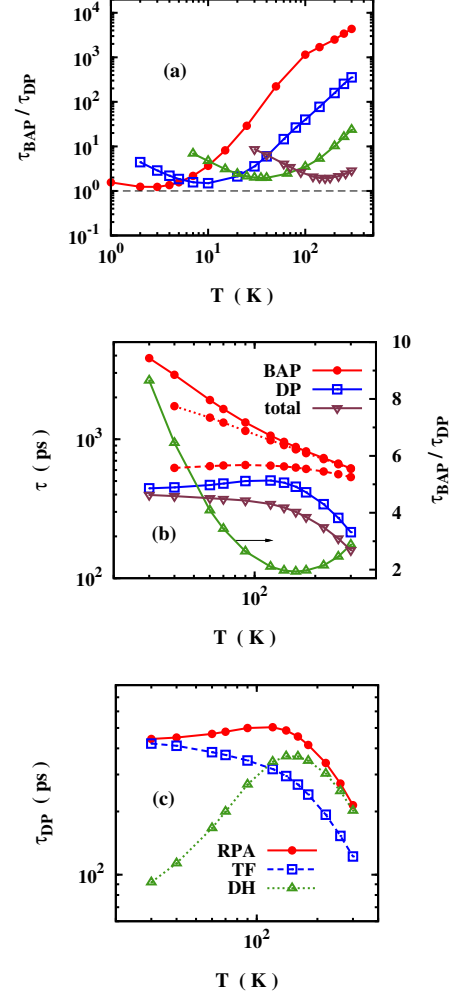


FIG. 10: (Color online) *p*-GaAs. Ratio of the SRT due to the BAP mechanism to that due to the DP mechanism as function of temperature for various hole densities with $N_{ex} = 0.1n_h$ and $n_i = n_h$. (a): $n_h = 3 \times 10^{15} \text{ cm}^{-3}$ (curve with \bullet), $3 \times 10^{16} \text{ cm}^{-3}$ (curve with \square), $3 \times 10^{17} \text{ cm}^{-3}$ (curve with \triangle), and $3 \times 10^{18} \text{ cm}^{-3}$ (curve with ∇). The hole Fermi temperatures for these densities are $T_{Fh} = 1.7, 7.7, 36,$ and 167 K , respectively. The electron Fermi temperatures are $T_F = 2.8, 13, 61,$ and 283 K , respectively. (b): The SRTs due to the BAP and DP mechanisms, the total SRT, together with the ratio $\tau_{\text{BAP}}/\tau_{\text{DP}}$ (curve with \triangle) versus the temperature for $n_h = 3 \times 10^{18} \text{ cm}^{-3}$. The dotted (dashed) curve represents the SRT due to the BAP mechanism without the Pauli blocking of electrons (holes). Note the scale of $\tau_{\text{BAP}}/\tau_{\text{DP}}$ is on the right hand side of the frame. (c): SRTs due to the DP mechanism with the TF (curve with \square), DH (curve with \triangle), and the RPA (curve with \bullet) screenings.

tio of the SRT due to the BAP mechanism to that due to the DP mechanism is plotted in Fig. 9(a) for various hole densities. It is seen that the DP mechanism dominates at high temperature, whereas the BAP mechanism dominates at low temperature, which is consistent with previous investigations.^{1,3,19,36,45} An interesting feature

is that the ratio first decreases rapidly, then slowly, and then again rapidly with decreasing temperature. A typical case is shown in Fig. 9(b) for $n_h = 3 \times 10^{18} \text{ cm}^{-3}$. It is noted that the “plateau” is around the hole Fermi temperature $T_{Fh} = 156 \text{ K}$ which is given by

$$T_{Fh} = \frac{(3\pi^2 n_h)^{2/3}}{2k_B m_0 \left[(\gamma_1 - 2\gamma_2)^{-3/2} + (\gamma_1 + 2\gamma_2)^{-3/2} \right]^{2/3}}. \quad (28)$$

The underlying physics is that: on one hand, the Pauli blocking of holes becomes important when $T \lesssim T_{Fh}$, which slows down the BAP spin relaxation effectively [see Eq. (20)]; on the other hand, the increase of the screening (mainly from holes) with decreasing temperature weakens the electron-impurity and carrier-carrier scatterings and thus enhances the DP spin relaxation. Consequently, the decrease of the ratio with decreasing temperature slows down and the “plateau” is formed around T_{Fh} . However, after the hole system enters the degenerate regime, the screening changes little with temperature. The ratio thus decreases rapidly with decreasing temperature again. We also plot the SRT due to the BAP mechanism without the Pauli blocking of holes as dotted curve in Fig. 9(b), which indicates that the Pauli blocking of holes effectively suppresses the BAP spin relaxation at low temperature ($T \lesssim T_{Fh}$). To elucidate the role of screening on DP spin relaxation, we plot the SRT due to the DP mechanism with the Thomas-Fermi (TF) screening⁷⁵ (which applies in the degenerate regime), the Debye-Huckle (DH) screening⁷⁵ (which applies in the non-degenerate regime), and the RPA screening in Fig. 9(c). The crossover of the screening from the DH to TF one is clearly seen in the figure. Also, compared to the temperature independent screening case (i.e., the TF screening case), one can see that the increase of the SRT with decreasing temperature is indeed slowed down around T_{Fh} due to the increase of screening. It is seen from Fig. 9(b) that the total SRT increases with decreasing temperature as both τ_{DP} and τ_{BAP} do.

We then discuss the case with high photo-excitation density, where we choose $N_{ex} = 0.1n_h$. The ratio of the SRT due to the BAP mechanism to that due to the DP mechanism is plotted in Fig. 10(a) for various hole densities. It is seen that, interestingly, the ratio is non-monotonic and has a minimum roughly around the Fermi temperature of electrons, $T \sim T_F$. The BAP mechanism is comparable with the DP mechanism only in the moderate temperature regime roughly around T_F , whereas for higher or lower temperature it becomes unimportant. To explore the underlying physics, we plot the SRTs due to the BAP and DP mechanisms in Fig. 10(b) and (c) for $n_h = 3 \times 10^{18} \text{ cm}^{-3}$. It is seen from Fig. 10(b) that the Pauli blocking of electrons and holes largely suppresses the BAP spin relaxation in the low temperature regime ($T \lesssim T_{Fh}$). Without the Pauli blocking, the SRT due to the BAP mechanism τ_{BAP} , and also the ratio τ_{BAP}/τ_{DP} , would saturate at low temperature when both the electron and hole systems are in the degenerate regime. It

should be mentioned that the electron Fermi temperature is larger than the hole one in these cases ($T_F = 1.7T_{Fh}$). Thus the crossover from non-degenerate regime to degenerate regime in the electron system takes place before that in the hole system. During the crossover in the hole system, the screening effect, which slows down the momentum scattering and enhances the DP spin relaxation, becomes significant as the screening is mainly from holes (both because $n_h > n_e$ and because the effective mass of heavy-hole is much larger than the electron one). It is seen from Fig. 10(c) that the SRT decreases monotonically with temperature for the TF screening, whereas for the DH screening and the RPA screening the SRT first increases then decreases with temperature. The decrease of the SRT at high temperature, where both the electron and hole systems are in the non-degenerate regime, is due to the rapid increase of the inhomogeneous broadening (varies as $\sim T^3$), whereas the increase of momentum scattering due to the decrease of screening is slower (varies as $\langle V_q^2 \rangle \propto 1/(q^2 + \kappa^2)^2 \lesssim 1/\kappa^4 \propto T^2$ as the screening constant $\kappa \propto T^{-1/2}$ in the non-degenerate regime). In the lower temperature regime where the electron system is in the degenerate regime and the hole system is still in the crossover regime, however, the inhomogeneous broadening varies with temperature slowly whereas the increase of the scattering due to the decrease of screening from holes with increasing temperature is dominant. Therefore, the SRT increases with temperature. Consequently, the peak is formed. It is found that the peak is roughly around T_F . Therefore, the minimum of the ratio τ_{BAP}/τ_{DP} is also roughly around T_F as τ_{BAP} always decreases with temperature. It should be noted that this peak is different from the peak found in intrinsic semiconductors in Sec. IV where the peak is due to the nonmonotonic temperature dependence of the electron-electron Coulomb scattering, whereas the main scattering mechanism here is the electron-impurity scattering. It is noted from the figure that in the further lower temperature regime where both the electron and hole systems are degenerate, the SRT due to the DP mechanism varies little with temperature. This is because both the inhomogeneous broadening and the momentum scattering (as well as the screening) change little with temperature when both the electron and hole systems are in the degenerate regime. It is seen from Fig. 10(b) that the total SRT increases rapidly with decreasing temperature in the high temperature regime but saturates at low temperature as τ_{DP} does.

For intermediate photo-excitation densities, τ_{BAP} always increases with decreasing temperature due to the Pauli blocking of electrons and holes. On the other hand, τ_{DP} first increases with decreasing temperature, then saturates at low temperature when the electron system is in the degenerate regime due to the fact that both the inhomogeneous broadening and the momentum scattering change little with temperature. Therefore, the ratio τ_{BAP}/τ_{DP} first decreases with decreasing temperature in the high temperature regime and then increases

in the low temperature regime when the electron system is degenerate because τ_{BAP} increases with decreasing temperature while τ_{DP} saturates. Consequently, the ratio $\tau_{\text{BAP}}/\tau_{\text{DP}}$ has a minimum in the crossover regime, roughly around T_F .

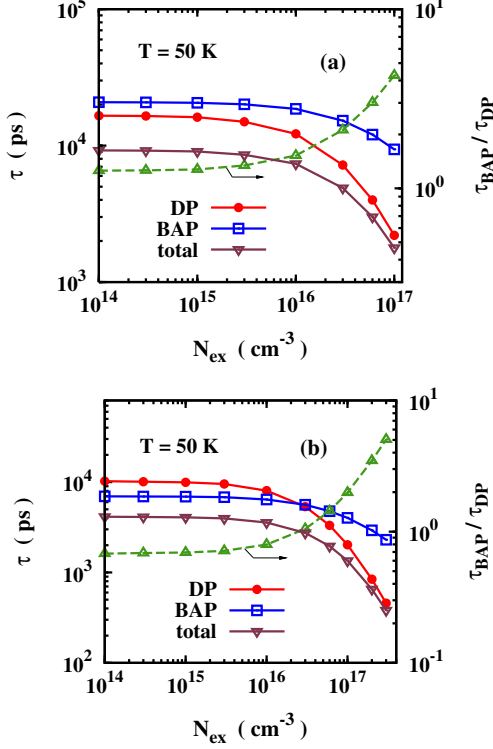


FIG. 11: (Color online) *p*-GaAs. SRTs τ due to the BAP and DP mechanisms together with the total SRT versus the photo-excitation density N_{ex} . The ratio of the two is plotted as dashed curve (note that the scale is on the right hand side of the frame). (a): $n_i = n_h = 3 \times 10^{17} \text{ cm}^{-3}$. (b): $n_i = n_h = 3 \times 10^{18} \text{ cm}^{-3}$. $T = 50 \text{ K}$.

We now turn to the photo-excitation density dependence of the SRT. In Fig. 11(a), we plot the SRT due to the DP mechanism and that due to the BAP mechanism as function of photo-excitation density for $n_h = 3 \times 10^{17} \text{ cm}^{-3}$ with $T = 50 \text{ K}$. It is seen that the SRT due to the DP mechanism decreases with the photo-excitation density monotonically. Specifically, it first decreases slowly, then ($N_{ex} > 10^{16} \text{ cm}^{-3}$) rapidly with the photo-excitation density. The scenario is as follows: In *p*-type semiconductors at low temperature, the dominant scattering mechanisms are the electron-hole and electron-impurity scatterings. The momentum scattering due to these two mechanism changes little with photo-excitation (electron) density ($N_{ex} = n_e$) for $N_{ex} < n_h$. In the low density regime ($n_e < 3 \times 10^{15} \text{ cm}^{-3}$, or $T_F < 13 \text{ K}$), where the electron system is non-degenerate, the increase of density affects the inhomogeneous broadening very little. Thus the SRT changes slowly with the photo-excitation density. In the high density regime ($n_e > 3 \times 10^{16} \text{ cm}^{-3}$, or $T_F > 61 \text{ K}$), the electron system is degenerate where

the inhomogeneous broadening increases fast with density. Consequently the SRT decreases rapidly with the photo-excitation density. For the SRT due to the BAP mechanism, it decreases slowly with the photo-excitation density in the low density regime, but rapidly in the high density regime. The decrease is mainly due to the increase of the averaged electron velocity $\langle v_k \rangle$ [see Eq. (20)], which is determined by the temperature and is insensitive to density in the non-degenerate regime, but increases rapidly in the degenerate regime. However, the increase of the spin relaxation due to the BAP mechanism is slower than that due to the DP mechanism, because the inhomogeneous broadening increases as $\propto N_{ex}^2$ while $\langle v_k \rangle$ increases as $\propto N_{ex}^{1/3}$. Consequently, the BAP mechanism becomes even less important in the high photo-excitation density regime. Similar situation also happens for other hole densities and temperatures. In Fig. 11(b), we plot the case for a larger hole density $n_h = 3 \times 10^{18} \text{ cm}^{-3}$. It is seen that under low photo-excitation, the BAP mechanism is more important than the DP mechanism. However, the BAP mechanism becomes less important than the DP mechanism in the high photo-excitation density regime. The crossover of the low photo-excitation density regime to the high photo-excitation density regime takes place around $T_F \sim T$. This leads to the conclusion that the BAP mechanism is not important at high photo-excitation density in *p*-type materials. It is seen from Fig. 11 that the total SRT decreases with photo-excitation density as both τ_{DP} and τ_{BAP} do.

We also study the hole density dependence of spin relaxation due to the BAP and DP mechanisms. In Fig. 12(a), we plot the SRT due to the BAP mechanism and that due to the DP mechanism as function of hole density for $T = 60 \text{ K}$ and $N_{ex} = 10^{14} \text{ cm}^{-3}$. It is seen that the SRT due to the BAP mechanism decreases as $1/n_h$ at low hole density, which is consistent with Eq. (19), i.e., for non-degenerate holes $\tau_{\text{BAP}} \propto 1/n_h$. At high hole density, τ_{BAP} decreases slower than $1/n_h$ due to the Pauli blocking of holes. However, for the SRT due to the DP mechanism, the dependence is not so obvious: the SRT first increases, then decreases and again increases with the hole density. As the electron distribution, and hence the inhomogeneous broadening, does not change with the hole density, the variation of the SRT due to the DP mechanism solely comes from the momentum scattering (mainly from the electron-impurity scattering). To elucidate the underlying physics, we plot the SRT due to the DP mechanism calculated with the RPA screening together with those calculated with the TF and DH screenings in Fig. 12(b). From the figure it is seen that the first increase and the decrease is connected with the DH screening, whereas the second increase is connected with the TF screening. The underlying physics is as follows: In the low hole density regime, the screening from the holes is small and the Coulomb potential, which is proportional to $1/(\kappa^2 + q^2)$, changes slowly with the screening constant κ . Hence the electron-impurity scattering increases with n_h as it is proportional to $n_i \langle V_q^2 \rangle \propto n_h$ (as $n_i = n_h$). For

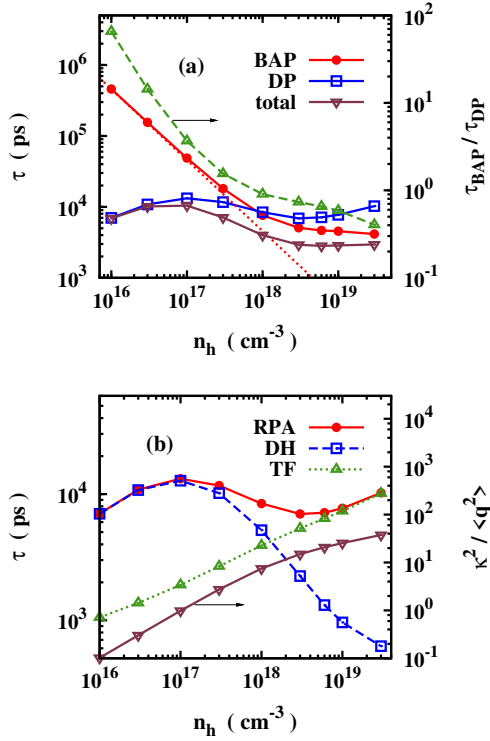


FIG. 12: (Color online) *p*-GaAs. (a): SRTs τ due to the BAP and DP mechanisms together with the total SRT against hole density n_h . $N_{\text{ex}} = 10^{14}$ cm $^{-3}$, $n_i = n_h$, and $T = 60$ K. The dotted curve denotes a fitting of the curve with \bullet using $1/n_h$ scale. The curve with \triangle denotes the ratio $\tau_{\text{BAP}}/\tau_{\text{DP}}$ (note that the scale is on the right hand side of the frame). (b): SRTs due to the DP mechanism with the DH (curve with \square), TF (curve with \triangle), and the RPA (curve with \bullet) screenings. The ratio $\kappa^2/\langle q^2 \rangle$ is plotted as curve with ∇ (note that the scale is on the right hand side of the frame).

higher hole density ($n_h > 10^{17}$ cm $^{-3}$), the screening constant κ becomes larger than the transferred momentum q . [To elucidate the relative ratio of the two, we plot the ratio of the average of the square of the transferred momentum $\langle q^2 \rangle$ to the square of the screening constant κ^2 as curve with ∇ in Fig. 12(b).] Hence the electron-impurity scattering decreases with n_h because it is proportional to $n_i \langle V_q^2 \rangle \propto n_h / \kappa^4 \propto n_h^{-1}$ as $\kappa^2 \propto n_h$ for the DH screening. As the hole density increases, the hole system enters into the degenerate regime, where the TF screening applies and $\kappa^2 \propto n_h^{1/3}$. Hence, the electron-impurity scattering increases with the hole density as $n_i \langle V_q^2 \rangle \propto n_h^{1/3}$. Consequently, the SRT first increases, then decreases and again increases with the hole density as the momentum scattering does. It should be mentioned that this behavior is different from that in the *p*-type (001) quantum wells where τ_{DP} increases with n_i monotonically⁷⁶ as the screening from holes is much weaker in that case due to lower-dimension in phase-space and smaller hole effective mass [in (001) GaAs quantum wells, the in-plane effective mass of the heavy-hole is $\sim 0.11m_0$ compared to $0.54m_0$

in bulk].

It is also noted in Fig. 12(a) that the ratio $\tau_{\text{BAP}}/\tau_{\text{DP}}$ first decreases rapidly, then slowly and again rapidly with the hole density n_h . The first decrease is because that τ_{BAP} decreases with n_h , whereas τ_{DP} increases with it. In the crossover regime ($n_h \sim 10^{18}$ cm $^{-3}$), where $T_F \sim T$, the SRT due to the DP mechanism varies slowly with hole density. As the SRT due to the BAP mechanism also varies slowly with hole density due to the Pauli blocking of holes, the ratio $\tau_{\text{BAP}}/\tau_{\text{DP}}$ changes slowly with hole density in this regime and a “plateau” is formed at $T_F \sim T$. In higher hole density regime, however, τ_{DP} increases with n_h , whereas τ_{BAP} decreases with it. The ratio $\tau_{\text{BAP}}/\tau_{\text{DP}}$ hence decreases rapidly with n_h again and the BAP mechanism becomes more and more important. It is seen from Fig. 12(a) that the total SRT first increases then decreases in the low hole density regime as τ_{DP} does. Nevertheless, in the regime of higher hole density, the total SRT changes slowly with n_h as the BAP and DP mechanisms compete with each other.

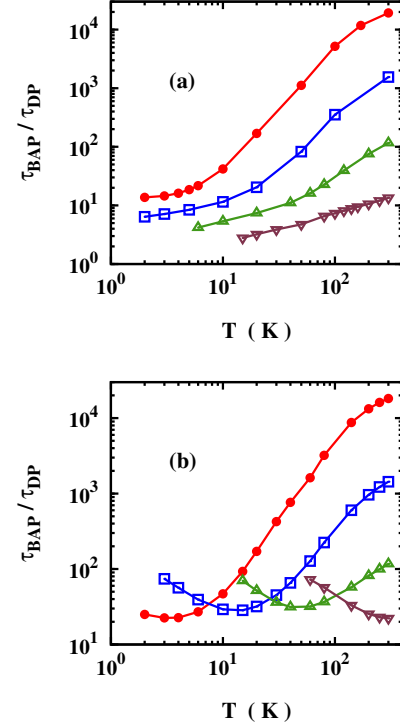


FIG. 13: (Color online) *p*-GaSb. Ratio of the SRT due to the BAP mechanism to that due to the DP mechanism as function of temperature for $n_h = 3 \times 10^{15}$ cm $^{-3}$ (curve with \bullet), 3×10^{16} cm $^{-3}$ (curve with \square), 3×10^{17} cm $^{-3}$ (curve with \triangle), and 3×10^{18} cm $^{-3}$ (curve with ∇). $n_i = n_h$. (a): $N_{\text{ex}} = 10^{14}$ cm $^{-3}$. (b): $N_{\text{ex}} = 0.1n_h$.

Although the above conclusions are obtained from GaAs, they also hold for other III-V semiconductors. To demonstrate that, we also investigate the problem in GaSb. GaSb is a narrow band gap III-V semiconductors of which the values of ΔE_{LT} and ΔE_{SR} can be found in

literature.^{45,58} In Fig. 13, we plot the ratio of the SRT due to the BAP mechanism to that due to the DP mechanism as function of temperature for various hole densities. It is seen from the figures that the features are similar to those in GaAs, whereas the ratio is much larger than that in GaAs under the same condition. That is, the relative importance of the BAP mechanism in GaSb is smaller than that in GaAs. This is because the SOC in GaSb is much larger than that in GaAs while the longitudinal-transversal splitting ΔE_{LT} in GaSb is smaller than that in GaAs.

VI. EFFECTS OF ELECTRIC FIELD ON SPIN RELAXATION IN *n*-TYPE III-V SEMICONDUCTORS

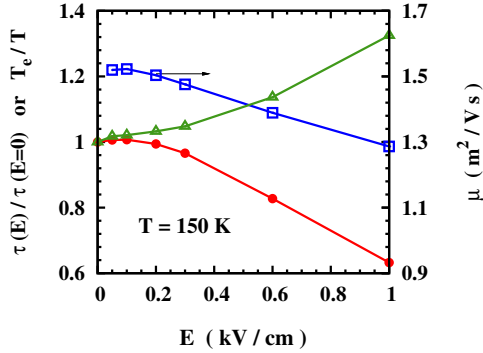


FIG. 14: (Color online) *n*-GaAs. Ratio of the SRT under electric field to the electric-field free one $\tau(E)/\tau(E=0)$ (curve with \bullet) and the ratio of the hot-electron temperature to the lattice temperature T_e/T (curve with \triangle) as function of electric field for $n_i = n_e = 2 \times 10^{17} \text{ cm}^{-3}$ at $T = 150 \text{ K}$. The mobility is also plotted as curve with \square (note that the scale is on the right hand side of the frame).

In this section, we study the effects of electric field on spin relaxation in *n*-type III-V semiconductors. Previous studies have demonstrated that in quantum wells a relatively high in-plane electric field can effectively manipulate the SRT.^{22,23,25,27} The underlying physics is that the high electric field induces two effects: the drift of the electron ensemble which enhances the inhomogeneous broadening (as electrons distribute on larger \mathbf{k} states where the SOC is larger), as well as the hot-electron effect which enhances the momentum scattering. The former tends to suppress while the latter tends to enhance the SRT. Thus the SRT has nonmonotonic electric field dependence: it first increases due to the hot-electron effect then decreases due to the enhancement of inhomogeneous broadening. In bulk semiconductors, the electric field dependence of spin lifetime has not been investigated. In this section, we present such a study. Using *n*-type GaAs as an example, we demonstrate that the electric field dependence of spin lifetime can be nonmonotonic (first in-

creasing then decreasing) or monotonic (decreasing) depending on the lattice temperature and the densities of impurities and electrons. The underlying physics is analyzed. The study indicates that the spin lifetime can be effectively controlled by electric field.

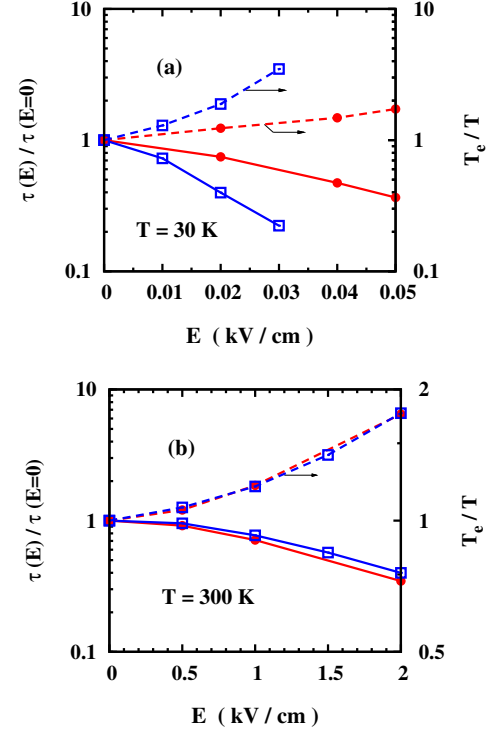


FIG. 15: (Color online) *n*-GaAs. Ratio of the SRT under electric field to the electric-field-free one $\tau(E)/\tau(E=0)$ (solid curves) and the ratio of the hot-electron temperature to the lattice temperature T_e/T (dashed curves) as function of electric field for (a): $T = 30 \text{ K}$ with $n_e = 10^{16} \text{ cm}^{-3}$ (curve with \bullet : $n_i = n_e$; curve with \square : $n_i = 0.05n_e$) and (b): $T = 300 \text{ K}$ with $n_e = n_i$ (curve with \bullet : $n_e = 10^{16} \text{ cm}^{-3}$; curve with \square : $n_e = 2 \times 10^{17} \text{ cm}^{-3}$).

In Fig. 14, we plot the ratio of the SRT under electric field to the electric-field-free one as function of electric field for $n_e = 2 \times 10^{17} \text{ cm}^{-3}$ with $P = 2\%$ at $T = 150 \text{ K}$ and $n_i = n_e$. The electric field is chosen to be along the x -axis and the initial spin polarization is along the z -axis. Due to the cubic form of the SOC, the average of the spin-orbit field is negligible even in the presence of finite center-of-mass drift velocity, which is different from the case in quantum wells where the linear \mathbf{k} -term gives a large effective magnetic field in the presence of electric field thanks to strong well confinement.^{22,27} It is seen that the ratio first increases a little and then decreases rapidly with the electric field. At $E = 1 \text{ kV/cm}$, the ratio drops to 0.6 which demonstrates that the electric field can effectively affect the SRT. To understand these effects, we also plot the hot-electron temperature in the figure. It is noted that the electron temperature increases first slowly then ($E > 0.3 \text{ kV/cm}$) rapidly with

the electric field, indicating clearly the hot-electron effect. For the two-dimension electron system, where the SOC is dominated by the linear term, the hot-electron effect mainly leads to the enhancement of scattering, whereas the enhancement of inhomogeneous broadening due to the hot-electron effect is marginal.²² Differently, the hot-electron effect also has important effect on inhomogeneous broadening in bulk system, as the SOC is cubic. As both the drift effect and the hot-electron effect increase the inhomogeneous broadening, the enhancement of the inhomogeneous broadening is faster than the increase of momentum scattering. Consequently, the SRT is easier to decrease with the electric field, which is different from the case of 2DES. We speculate that the electric field dependence of the SRT in Wurtzite semiconductors and strained III-V semiconductors resembles that in the GaAs quantum wells, when the SOC is dominated by the linear \mathbf{k} term.^{11,39,77} The mobility of the electron system is also plotted in the figure. The variation of the mobility indicates the nonlinear effects of the electric field in the kinetics of electron system.

For lower and higher temperature cases, we plot the results in Fig. 15. The electron density is $n_e = 10^{16} \text{ cm}^{-3}$ in Fig. 15(a). It is seen that the ratio for the case with low impurity density $n_i = 0.05n_e$ decreases faster than that for the case with $n_i = n_e$. This is because both the hot-electron effect and the drift effect are more pronounced in cleaner system,²² which thus leads to a faster decrease of the SRT due to the enhancement of inhomogeneous broadening. In the background of hot-electron spin injection under high bias, our results indicate that the manipulation of the SRT by the electric field is more pronounced for samples with high mobility. For high temperature case ($T = 300 \text{ K}$), we plot the SRT and hot-electron temperature as function of electric field for two different electron densities $n_e = 10^{16} \text{ cm}^{-3}$ and $n_e = 2 \times 10^{17} \text{ cm}^{-3}$ with $n_i = n_e$ in Fig. 15(b). It is seen that both the SRT and the electron temperature differs marginally for the two cases even though their impurity and electron densities differ by 20 times. This is because that at 300 K the electron-LO-phonon scattering is more important than the electron-impurity scattering. Thus both the drift of the electron system and the hot-electron effect is mainly determined by the electron-LO-phonon scattering, and the variation of the SRT with electric field is insensitive to impurity density. For electron density, as the electron system is in the non-degenerate regime for both cases, the electron density dependence is hence also weak.

VII. CONCLUSION

In conclusion, we have applied an efficient scheme, the fully microscopic KSBEs, to study the spin dynamics in bulk III-V semiconductors, with all scattering explicitly included. This approach takes full account of the spin relaxation due to the DP, EY, and BAP mechanisms in a fully microscopic fashion, and enables us to find impor-

tant results missing in the previous simplified approaches in the literature. From the KSBE approach, we study the electron spin relaxation in n -type, intrinsic, and p -type III-V semiconductors. We also investigate the effects of electric field on spin relaxation in n -type III-V semiconductors.

For n -type III-V semiconductors, differing from the previous conclusions, we find that the spin relaxation due to the EY mechanism is less important than that due to the DP mechanism even in narrow band-gap semiconductors, such as InAs and InSb. We then focus on the spin relaxation due to the DP mechanism. We find that the density dependence of the SRT is nonmonotonic and we predict a peak which appears in the metallic regime. This behavior is due to the different density dependences of the inhomogeneous broadening and the momentum scattering in the degenerate and non-degenerate regimes. In the non-degenerate regime, as the electron distribution is close to the Boltzmann distribution, the inhomogeneous broadening changes little with the density but the electron-electron and electron-impurity scatterings increase with the electron density. As a result, the SRT increases with the density. In the degenerate regime, the inhomogeneous broadening increases with electron density, whereas the momentum scatterings decrease with it. Consequently, the SRT decreases with the electron density in the degenerate regime. The peak of the SRT is hence formed in the crossover regime, where the corresponding Fermi temperature is close to the lattice temperature, $T_F \sim T$. Our results show that the electron-electron scattering plays an important role in the spin relaxation. We also study the density dependence for the case with strain-induced SOC, where the density dependence of the inhomogeneous broadening is different as the linear \mathbf{k} -dependence of the SOC plays important role. However, the SRT still has a peak but at a larger density compared to the strain-free case. We further study the temperature dependence of the SRT. We find that the SRT decreases monotonically with the temperature which is consistent with experimental findings. After we artificially lower the impurity density, we find a peak in the SRT which is due to the different temperature dependence of the electron-electron scattering in the degenerate and non-degenerate regimes. This is consistent with the results in 2DES where the peak in the SRT due to the electron-electron scattering appears only when the impurity density is low (e.g., $n_i = 0.1n_e$).²⁵ We also study the initial spin polarization dependence of the SRT where the effect of the Coulomb HF term is discussed. We find that the dependence is quite weak in bulk system compared to that in the 2DES, which is again due to the large impurity density $n_i \geq n_e$ in bulk system.

For intrinsic III-V semiconductors, we first compare the BAP mechanism and the DP mechanism. We find that the BAP mechanism is far less efficient than the DP mechanism. We further compare our results from the fully microscopic KSBE approach with those from the approach widely used in the literature. We find

that the previous approach deviates in the low temperature regime due to the preemption of the Pauli blocking. Also, the previous approach ignores the long-range electron-hole exchange scattering which is shown to be dominant in GaAs. We find that the electron-hole Coulomb scattering plays an important role in spin relaxation. The Coulomb HF term is found to have important effects on spin relaxation at low temperature and high photo-excitation density, as the impurity density is very low in intrinsic semiconductors (we choose $n_i = 0$). Due to the same reason, the peak in the temperature dependence of the SRT due to the electron-electron scattering also appears at small spin polarization. We further discuss the photo-excitation density dependence of the SRT. We find that the SRT first increases then decreases with the density which resembles the case in n -type samples where the underlying physics is also similar.

For p -type III-V semiconductors, we first examine the relative importance of the BAP mechanism. We find that the BAP mechanism dominates the spin relaxation in the low temperature regime only when the photo-excitation density is low. However, when the photo-excitation density is high, the BAP mechanism can be comparable with the DP mechanism only in the moderate temperature regime roughly around the Fermi temperature of electrons, whereas for higher or lower temperature it is unimportant. The photo-excitation density dependence of SRTs due to the BAP and DP mechanisms are also discussed. We find that the relative importance of the BAP mechanism decreases with photo-excitation density and eventually becomes negligible at sufficiently high photo-excitation density. For hole density dependence at small photo-excitation density, we find that the spin relaxation due to the BAP mechanism increases with hole density linearly in low hole density regime but the increase becomes slower in high hole density regime where the Pauli blocking of holes becomes important. Interestingly, the SRT due to the DP mechanism first increases, then decreases and again increases with hole density. The underlying physics is that the momentum scattering (mainly from the electron-impurity scattering) first increases with hole (impurity) ($n_i = n_h$) density, then decreases with hole density due to the increase of the screening. However, at high hole density when the hole system is degenerate, the screening increases slower with the hole density and the momentum scattering again increases with the hole (impurity) density. On the other hand, the inhomogeneous broadening does not change with hole density as the electron density is solely determined by the photo-excitation density. Consequently, the SRT due to the DP mechanism first increases, then decreases and again increases with the hole density. This behavior makes the ratio $\tau_{\text{BAP}}/\tau_{\text{DP}}$ first decreases rapidly, then slowly and again rapidly with the hole density. The BAP mechanism is more important than the DP one for high hole density. The relative importance of the BAP mechanism in GaSb is found to be much less than that in GaAs due to both the weaker electron-hole exchange interaction and

the larger SOC in GaSb.

Finally, we study the effect of electric field on the spin relaxation in n -type GaAs. We find that the SRT can be largely affected by the electric field. The underlying physics is that the electric field induces two effects: the center-of-mass drift which enhances the inhomogeneous broadening and the hot-electron effect which increases both the momentum scattering and the inhomogeneous broadening. The electric field dependence of SRT thus can be nonmonotonic: it first increases due to the increase of scattering then decreases due to the enhancement of inhomogeneous broadening. However, we find that differing from the 2DES, the SRT is easier to decrease with the electric field. This is because that the inhomogeneous broadening increases faster when the SOC is cubic compared to the 2DES where the SOC is dominated by linear \mathbf{k} term. We expect that the electric field dependence of the SRT resembles the 2DES for Wurtzite semiconductors or strained semiconductors, where the SOC can be dominated by the linear \mathbf{k} term. We also find that the effect of the electric field becomes more significant for low impurity density samples at low temperature as both the drift effect and the hot-electron effect are more pronounced. However, at room temperature, the effect of the electric field is insensitive to the impurity density as the electron-LO-phonon scattering is more important than the electron-impurity scattering. The electron density dependence is also weak as long as the system is in the non-degenerate regime.

Acknowledgments

This work was supported by the Natural Science Foundation of China under Grant No. 10725417, the National Basic Research Program of China under Grant No. 2006CB922005, and the Knowledge Innovation Project of Chinese Academy of Sciences. One of the author (J.H.J.) would like to thank M. Q. Weng and K. Shen for discussions.

APPENDIX A: COMPARISON WITH EXPERIMENT

We compare the calculation from the fully microscopic KSBE approach with the experimental result in Ref. 4 for n -type GaAs with $n_e = 10^{16} \text{ cm}^{-3}$. In Fig. 16, we plot the SRT as function of temperature from our calculation together with the experimental data. It is seen that the calculation agrees well with the experimental results for $T \gtrsim 20 \text{ K}$. The deviation in the lower temperature regime is due to the rising of the localization of electrons.^{6,16,17} The SRT due to the EY mechanism is also calculated, which is much larger than the experimental data, indicating the irrelevance of the EY mechanism. The calculation gives a fit of the SOC parameter as $\gamma_D = 8.2 \text{ eV} \cdot \text{\AA}^3$ which is different from the value

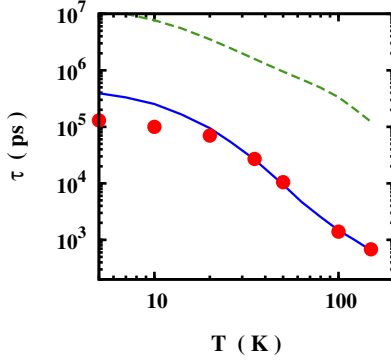


FIG. 16: (Color online) n -GaAs. SRTs τ from the experimental data in Ref. 4 (●) and from the calculation via the KSBE approach with only the DP mechanism (solid curve) as well as that with only the EY mechanism (dashed curve).

$\gamma_D = 23.9 \text{ eV} \cdot \text{\AA}^3$ calculated from the tight-binding or $\mathbf{k} \cdot \mathbf{p}$ parametric theories.^{56,57}

The SRT in GaAs due to the DP mechanism is calculated with $\gamma_D = 23.9 \text{ eV} \cdot \text{\AA}^3$ throughout the paper unless in Sec. V where we use $\gamma_D = 8.2 \text{ eV} \cdot \text{\AA}^3$ in order to avoid possible exaggeration of the DP mechanism by using a “larger” SOC parameter. However, the SRT due to the DP mechanism is proportional to γ_D^2 , thus the results presented in the paper can be easily converted to the results for another γ_D . The ratio for the SRTs in the two cases is 8.5.

APPENDIX B: NUMERICAL SCHEME

Our numerical scheme is based on the discretization of the \mathbf{k} -space similar to that in Ref. 22. The \mathbf{k} -space is divided into $N \times M \times L$ control regions where the \mathbf{k} -grid points are chosen to be $\mathbf{k}_{n,m,l} = \sqrt{2m_c E_n} (\sin \theta_m \cos \phi_l, \sin \theta_m \sin \phi_l, \cos \theta_m)$. To facilitate the evaluation of the δ -functions in the scattering terms, we set $E_n = (n + 1/2)\Delta E$, where the energy span in each control region is $\Delta E = \omega_{LO}/n_{LO}$ with n_{LO} being an integer number and ω_{LO} denoting the LO-phonon frequency. The electron-impurity and electron-phonon scatterings are then solved easily since the δ -functions can be integrated out directly.

For the electron-electron Coulomb, electron-hole Coulomb and electron-hole exchange scatterings, the situation is much more complex. The electron-electron Coulomb scattering term [Eq. (9)] can be rewritten as,

$$\begin{aligned} \partial_t \hat{\rho}_{\mathbf{k}}|_{ee} = & \sum_{\mathbf{k}'} \frac{-\pi}{(2\pi)^3} V_{\mathbf{k}-\mathbf{k}'} [\hat{\Lambda}_{\mathbf{k},\mathbf{k}'} \hat{\rho}_{\mathbf{k}'}^> \hat{\Lambda}_{\mathbf{k}',\mathbf{k}} \hat{\rho}_{\mathbf{k}}^< H(\mathbf{k}, \mathbf{k}') \\ & - \hat{\Lambda}_{\mathbf{k},\mathbf{k}'} \hat{\rho}_{\mathbf{k}'}^< \hat{\Lambda}_{\mathbf{k}',\mathbf{k}} \hat{\rho}_{\mathbf{k}}^> H(\mathbf{k}', \mathbf{k})] + \text{H.c.}, \quad (\text{B1}) \end{aligned}$$

where

$$\begin{aligned} H(\mathbf{k}, \mathbf{k}') = & (2\pi)^3 \sum_{\mathbf{k}''} \delta(\varepsilon_{\mathbf{k}''} - \varepsilon_{\mathbf{k}''-\mathbf{k}+\mathbf{k}'} + \varepsilon_{\mathbf{k}'} - \varepsilon_{\mathbf{k}}) \\ & \times \text{Tr} \left(\hat{\Lambda}_{\mathbf{k}'',\mathbf{k}''-\mathbf{k}+\mathbf{k}'} \hat{\rho}_{\mathbf{k}''-\mathbf{k}+\mathbf{k}'}^< \hat{\Lambda}_{\mathbf{k}''-\mathbf{k}+\mathbf{k}',\mathbf{k}''} \hat{\rho}_{\mathbf{k}''}^> \right). \quad (\text{B2}) \end{aligned}$$

Substituting $\mathbf{q} = \mathbf{k} - \mathbf{k}'$ and $\omega = 2m_c(\varepsilon_{\mathbf{k}} - \varepsilon_{\mathbf{k}'})$, one has

$$\begin{aligned} H(\mathbf{q}, \omega) = & \int d\mathbf{k}'' \delta(\varepsilon_{\mathbf{k}''} - \varepsilon_{\mathbf{k}''-\mathbf{q}} - \omega/2m_c) \\ & \times \text{Tr} \left(\hat{\Lambda}_{\mathbf{k}'',\mathbf{k}''-\mathbf{q}} \hat{\rho}_{\mathbf{k}''-\mathbf{q}}^< \hat{\Lambda}_{\mathbf{k}''-\mathbf{q},\mathbf{k}''} \hat{\rho}_{\mathbf{k}''}^> \right). \quad (\text{B3}) \end{aligned}$$

Now the δ function can be simplified as

$$\delta(\varepsilon_{\mathbf{k}''} - \varepsilon_{\mathbf{k}''-\mathbf{q}} - \omega/2m_c) = \frac{m_c}{k''q} \delta(\cos \hat{\theta} - \cos \hat{\theta}_0), \quad (\text{B4})$$

where $\hat{\theta}$ is the angle between \mathbf{k}'' and \mathbf{q} , and $\cos \hat{\theta}_0 = (q^2 + \omega)/2k''q$. To evaluate the δ function, it is helpful to rotate to the new coordinate with \mathbf{q} being along the z -axis. In this coordinate, $\hat{\theta} = \theta$ and the δ function can be evaluated readily. The result is

$$\begin{aligned} H(\mathbf{q}, \omega) = & \frac{m_c^2}{q} \int d\varepsilon_{\mathbf{k}''} d\phi'' \\ & \times \text{Tr} \left(\hat{\Lambda}_{\mathbf{k}'',\mathbf{k}''-\mathbf{q}} \hat{\rho}_{\mathbf{k}''-\mathbf{q}}^< \hat{\Lambda}_{\mathbf{k}''-\mathbf{q},\mathbf{k}''} \hat{\rho}_{\mathbf{k}''}^> \right) \Big|_{\theta=\theta_0}^{(new)}, \quad (\text{B5}) \end{aligned}$$

with $\theta_0 = \arccos[(q^2 + \omega)/2k''q]$. Note that the integration over $\varepsilon_{\mathbf{k}''}$ is restrained by the condition $\varepsilon_{\mathbf{k}''} \geq [(q^2 + \omega)/2q]^2/2m_c$ according to $|\cos \theta_0| \leq 1$. Now the electron-electron Coulomb scattering is easily integrated out. Note that the calculation of $H(\mathbf{q}, \omega)$ can be done before the calculation of the electron-electron Coulomb scattering terms, which thus reduces the whole calculation complexity from $O(N^2 M^3 L^3)$ to $O(N^2 M^2 L^2)$. This method, first developed by Cheng,⁷⁸ greatly reduces the calculation complexity.

For the electron-hole Coulomb scattering, the idea is similar, but the technique is more complex. Denoting $x_m = m_c/m_m^*$, the δ -function in Eq. (10) can be written as

$$\begin{aligned} \delta(\varepsilon_{\mathbf{k}''m}^h - \varepsilon_{\mathbf{k}''-\mathbf{q}m'}^h - \omega/2m_c) = & 2m_c \\ & \times \delta \left((x_m - x_{m'}) k''^2 - x_{m'} q^2 + 2x_{m'} k'' q \cos \hat{\theta} - \omega \right). \quad (\text{B6}) \end{aligned}$$

The δ -function is then integrated out by similar means,

$$\begin{aligned} H_{eh}(\mathbf{q}, \omega) = & \sum_{m,m'} \frac{m_c^2}{q x_m x_{m'}} \int d\varepsilon_{\mathbf{k}''} d\phi'' |\mathcal{T}_{\mathbf{k}''-\mathbf{q}m'}^{\mathbf{k}''m}|^2 \\ & \times f_{\mathbf{k}''-\mathbf{q}m'}^h (1 - f_{\mathbf{k}''m}^h) \Big|_{\theta=\theta_0}^{(new)}. \quad (\text{B7}) \end{aligned}$$

The integration over $\varepsilon_{\mathbf{k}''}$ is restrained by the condition $|\cos \theta_0| \leq 1$, where

$$\cos \theta_0 = \frac{1}{2k''q} \left(\frac{\omega}{x_{m'}} + q^2 - \frac{x_m - x_{m'}}{x_{m'}} k''^2 \right). \quad (\text{B8})$$

The restriction can be simplified as

$$b^2 k''^2 - (1 + 2ab)k'' + a^2 \leq 0 \quad \text{and} \quad k'' \geq 0, \quad (\text{B9})$$

where $a = (\frac{\omega}{x_{m'}} + q^2)/2q$ and $b = (x_m - x_{m'})/2x_{m'}q$. The above inequality can be worked out readily for given (q, ω, m, m') , and the restriction condition for $\varepsilon_{\mathbf{k}''}^h = x_m k''^2/2m_c$ is then obtained.

The electron-hole exchange scattering is solved similarly by substituting the matrix element $|\mathcal{T}_{\mathbf{k}''-\mathbf{q}m'}^{\mathbf{k}''m}|^2$ with

$|\mathcal{J}_{\mathbf{k}''-\mathbf{q}m'}^{(\pm) \mathbf{k}''m}|^2$. Finally, the drift term is solved with similar method of that in Ref. 22. The differential equations are solved by the fourth-order Runge-Kutta method.

The computation is carried out in a parallel manner by using OpenMP. For a typical calculation with the partition of $40 \times 8 \times 16$ grid points in the \mathbf{k} -space, it takes about ten hours to evolve 50 ps on a quad-core AMD Phenom 9750.

-
- * Author to whom correspondence should be addressed; Electronic address: mwwwu@ustc.edu.cn.
 † Mailing Address
¹ F. Meier and B. P. Zakharchenya, *Optical Orientation* (North-Holland, Amsterdam, 1984).
² S. A. Wolf, D. D. Awschalom, R. A. Buhrman, J. M. Daughton, S. von Molnár, M. L. Roukes, A. Y. Chtchelkanova, and D. M. Treger, *Science* **294**, 1488 (2001).
³ *Semiconductor Spintronics and Quantum Computation*, ed. by D. D. Awschalom, D. Loss, and N. Samarth (Springer-Verlag, Berlin, 2002); I. Žutić, J. Fabian, and S. Das Sarma, *Rev. Mod. Phys.* **76**, 323 (2004); J. Fabian, A. Matos-Abiague, C. Ertler, P. Stano, and I. Žutić, *Acta Phys. Slov.* **57**, 565 (2007); *Spin Physics in Semiconductors*, ed. by M. I. D'yakonov (Springer, Berlin, 2008), and references therein.
⁴ J. M. Kikkawa and D. D. Awschalom, *Phys. Rev. Lett.* **80**, 4313 (1998).
⁵ J. M. Kikkawa and D. D. Awschalom, *Nature* **397**, 139 (1999).
⁶ J. M. Kikkawa and D. D. Awschalom, *Science* **287**, 473 (2000).
⁷ M. Oestreich, M. Bender, J. Hübner, D. Hägele, W. W. Rühle, Th. Hartmann, P. J. Klar, W. Heimbrodt, M. Lampalzer, K. Volz, and W. Stolz, *Semicond. Sci. Technol.* **17**, 285 (2002).
⁸ I. Malajovich, J. M. Kikkawa, D. D. Awschalom, J. J. Berry, and N. Samarth, *Phys. Rev. Lett.* **84**, 1015 (2000).
⁹ J. A. Gupta, R. Knobel, N. Samarth, and D. D. Awschalom, *Science* **292**, 2458 (2001).
¹⁰ Y. Kato, R. C. Myers, D. C. Driscoll, A. C. Gossard, J. Levy, and D. D. Awschalom, *Science* **299**, 1201 (2003).
¹¹ Y. Kato, R. C. Myers, A. C. Gossard, and D. D. Awschalom, *Nature* **427**, 50 (2004).
¹² L. Meier, G. Salis, I. Shorubalko, E. Gini, S. Schön, and K. Ensslin, *Nat. Phys.* **3**, 650 (2007).
¹³ Y. Yafet, *Phys. Rev.* **85**, 478 (1952); R. J. Elliot, *Phys. Rev.* **96**, 266 (1954).
¹⁴ M. I. D'yakonov and V. I. Perel', *Zh. Éksp. Teor. Fiz.* **60**, 1954 (1971) [*Sov. Phys. JETP* **33**, 1053 (1971)]; *Fiz. Tverd. Tela (Leningrad)* **13**, 3581 (1971) [*Sov. Phys. Solid State* **13**, 3023 (1972)].
¹⁵ G. L. Bir, A. G. Aronov, and G. E. Pikus, *Zh. Éksp. Teor. Fiz.* **69**, 1382 (1975) [*Sov. Phys. JETP* **42**, 705 (1976)].
¹⁶ R. I. Dzhirov, K. V. Kavokin, V. L. Korenev, M. V. Lazarev, B. Y. Meltser, M. N. Stepanova, B. P. Zakharchenya, D. Gammon, and D. S. Katzer, *Phys. Rev. B* **66**, 245204 (2002).

- ¹⁷ Z. Chen, S. G. Carter, R. Bratschitsch, P. Dawson, and S. T. Cundiff, *Nat. Phys.* **3**, 265 (2007).
¹⁸ Y. V. Pershin and V. Privman, *Nano Lett.* **3**, 695 (2003).
¹⁹ P. H. Song and K. W. Kim, *Phys. Rev. B* **66**, 035207 (2002).
²⁰ M. W. Wu and C. Z. Ning, *Eur. Phys. J. B* **18**, 373 (2000); M. W. Wu and H. Metiu, *Phys. Rev. B* **61**, 2945 (2000); M. W. Wu, *J. Phys. Soc. Jpn.* **70**, 2195 (2001).
²¹ M. Q. Weng and M. W. Wu, *Phys. Rev. B* **68**, 075312 (2003).
²² M. Q. Weng, M. W. Wu, and L. Jiang, *Phys. Rev. B* **69**, 245320 (2004).
²³ M. Q. Weng and M. W. Wu, *Phys. Rev. B* **70**, 195318 (2004).
²⁴ C. Lü, J. L. Cheng, and M. W. Wu, *Phys. Rev. B* **73**, 125314 (2006).
²⁵ J. Zhou, J. L. Cheng, and M. W. Wu, *Phys. Rev. B* **75**, 045305 (2007).
²⁶ J. Zhou and M. W. Wu, *Phys. Rev. B* **77**, 075318 (2008).
²⁷ P. Zhang, J. Zhou, and M. W. Wu, *Phys. Rev. B* **77**, 235323 (2008).
²⁸ J. H. Jiang, M. W. Wu, and Y. Zhou, *Phys. Rev. B* **78**, 125309 (2008).
²⁹ M. M. Glazov and E. L. Ivchenko, *Zh. Éksp. Teor. Fiz.* **126**, 1465 (2004) [*JETP* **99**, 1279 (2004)]; *Pis'ma Zh. Éksp. Teor. Fiz.* **75**, 476 (2002) [*JETP Lett.* **75**, 403 (2002)].
³⁰ W. J. Leyland, G. H. John, R. T. Harley, M. M. Glazov, E. L. Ivchenko, D. A. Ritchie, I. Farrer, A. J. Shields, and M. Henini, *Phys. Rev. B* **75**, 165309 (2007).
³¹ X. Z. Ruan, H. H. Luo, Y. Ji, Z. Y. Xu, and V. Umansky, *Phys. Rev. B* **77**, 193307 (2008).
³² L. H. Teng, P. Zhang, T. S. Lai, and M. W. Wu, *Europhys. Lett.* **84**, 27006 (2008).
³³ For brief review, see M. W. Wu, M. Q. Weng, and J. L. Cheng, in *Physics, Chemistry and Application of Nanostructures: Reviews and Short Notes to Nanomeeting 2007*, eds. V. E. Borisenko, V. S. Gurin, and S. V. Gaponenko (World Scientific, Singapore, 2007) p. 14, and references therein.
³⁴ D. Stich, J. Zhou, T. Korn, R. Schulz, D. Schuh, W. Wegscheider, M. W. Wu, and C. Schüller, *Phys. Rev. Lett.* **98**, 176401 (2007); *Phys. Rev. B* **76**, 205301 (2007).
³⁵ T. Korn, D. Stich, R. Schulz, D. Schuh, W. Wegscheider, and C. Schüller, arXiv:0811.0720.
³⁶ G. Fishman and G. Lampel, *Phys. Rev. B* **16**, 820 (1977).
³⁷ K. Zerrouati, F. Fabre, G. Bacquet, J. Bandet, J. Frandon, G. Lampel, and D. Paget, *Phys. Rev. B* **37**, 1334 (1988).
³⁸ P. Zhang and M. W. Wu, *Phys. Rev. B* **76**, 193312 (2007).

- ³⁹ L. Jiang and M. W. Wu, Phys. Rev. B **72**, 033311 (2005).
- ⁴⁰ D. Stich, J. H. Jiang, T. Korn, R. Schulz, D. Schuh, W. Wegscheider, M. W. Wu, and C. Schüller, Phys. Rev. B **76**, 073309 (2007).
- ⁴¹ A. W. Holleitner, V. Sih, R. C. Myers, A. C. Gossard, and D. D. Awschalom, New J. Phys. **9**, 342 (2007).
- ⁴² F. Zhang, H. Z. Zheng, Y. Ji, J. Liu, and G. R. Li, Europhys. Lett. **83**, 47006 (2008).
- ⁴³ F. Zhang, H. Z. Zheng, Y. Ji, J. Liu, and G. R. Li, Europhys. Lett. **83**, 47007 (2008).
- ⁴⁴ M. W. Wu and C. Z. Ning, Phys. Stat. Sol. (b) **222**, 523 (2000).
- ⁴⁵ A. G. Aronov, G. E. Pikus, and A. N. Titkov, Zh. Eksp. Teor. Fiz. **84**, 1170 (1983) [Sov. Phys. JETP **57**, 680 (1983)].
- ⁴⁶ I. Malajovich, J. J. Berry, N. Samarth, and D. D. Awschalom, Nature **411**, 770 (2000).
- ⁴⁷ H. Haug and A. P. Jauho, *Quantum Kinetics in Transport and Optics of Semiconductors* (Springer, Berlin, 1996).
- ⁴⁸ G. Dresselhaus, Phys. Rev. **100**, 580 (1955).
- ⁴⁹ D. J. Hilton and C. L. Tang, Phys. Rev. Lett. **89**, 146601 (2002).
- ⁵⁰ M. Krauß, M. Aeschlimann, and H. C. Schneider, Phys. Rev. Lett. **100**, 256601 (2008).
- ⁵¹ G. D. Mahan, *Many-Particle Physics* (Plenum Press, New York, 1990).
- ⁵² J. Schliemann, Phys. Rev. B **74**, 045214 (2006).
- ⁵³ M. Z. Maialle, E. A. de Andrada e Silva, and L. J. Sham, Phys. Rev. B **47**, 15776 (1993).
- ⁵⁴ *Semiconductors*, Landolt-Börnstein, New Series, Vol. 17a, ed. by O. Madelung (Springer-Verlag, Berlin, 1987).
- ⁵⁵ W. Ekardt, K. Lösch, and D. Bimberg, Phys. Rev. B **20**, 3303 (1979).
- ⁵⁶ J. Y. Fu, M. Q. Weng, and M. W. Wu, Physica E **40**, 2890 (2008).
- ⁵⁷ J.-M. Jancu, R. Scholz, E. A. de Andrada e Silva, and G. C. La Rocca, Phys. Rev. B **72**, 193201 (2005).
- ⁵⁸ U. Rössler and H.-R. Trebin, Phys. Rev. B **23**, 1961 (1981).
- ⁵⁹ A. Amo, L. Viña, P. Lugli, C. Tejedor, A. I. Toropov, and K. S. Zhuravlev, Phys. Rev. B **75**, 085202 (2007).
- ⁶⁰ J. N. Chazalviel, Phys. Rev. B **11**, 1555 (1975).
- ⁶¹ The spin-orbit parameter is another quantity which may affect the ratio. To check the parameter we used, we calculate the SRT corresponding to that measured in a recent experiment [P. Murzyn, C. R. Pidgeon, P. J. Phillips, J.-P. Wells, N. T. Gordon, T. Ashley, J. H. Jefferson, T. M. Burke, J. Giess, M. Merrick, B. N. Murdin, and C. D. Maxey, Phys. Rev. B **67**, 235202 (2003)], where $n_e = 2 \times 10^{15} \text{ cm}^{-3}$ and $N_{ex} = 10^{16} \text{ cm}^{-3}$ at 150 K. We get a SRT of 15.2 ps which is close to the measured value of 16 ps.
- ⁶² The spin-orbit parameter is also checked by comparing with the experimental results in Ref. 65. A best fitting gives $\gamma_D = 99.2$ in InAs which is 2.3 times as large as that in Ref. 57. This only enhances the DP spin relaxation and strengthens our conclusion that the EY mechanism is less efficient than the DP mechanism in InAs.
- ⁶³ K. L. Litvinenko, L. Nikzad, J. Allam, B. N. Murdin, C. R. Pidgeon, J. J. Harris, and L. F. Cohen, J. Supercon. **20**, 461 (2007).
- ⁶⁴ G. F. Giuliani and G. Vignale, *Quantum Theory of the Electron Liquid* (Cambridge University Press, Cambridge, 2005).
- ⁶⁵ B. N. Murdin, K. Litvinenko, J. Allam, C. R. Pidgeon, M. Bird, K. Morrison, T. Zhang, S. K. Clowes, W. R. Branford, J. Harris, and L. F. Cohen, Phys. Rev. B **72**, 085346 (2005).
- ⁶⁶ K. L. Litvinenko, B. N. Murdin, J. Allam, C. R. Pidgeon, T. Zhang, J. J. Harris, L. F. Cohen, D. A. Eustace, and D. W. McComb, Phys. Rev. B **74**, 075331 (2006).
- ⁶⁷ P. E. Hohage, G. Bacher, D. Reuter, and A. D. Wieck, Appl. Phys. Lett. **89**, 231101 (2006).
- ⁶⁸ H. Saarikoski and G. E. W. Bauer, arXiv:0810.3386.
- ⁶⁹ As demonstrated in Sec. V, the BAP mechanism is more important in GaAs than in GaSb, thus in GaSb the BAP mechanism is also negligible. Also a recent experimental investigation indicates that the BAP mechanism is unimportant in intrinsic InSb [B. N. Murdin, K. Litvinenko, D. G. Clarke, C. R. Pidgeon, P. Murzyn, P. J. Phillips, D. Carder, G. Berden, B. Redlich, A. F. G. van der Meer, S. Clowes, J. J. Harris, L. F. Cohen, T. Ashley, and L. Buckle, Phys. Rev. Lett. **96**, 096603 (2006)].
- ⁷⁰ Note that the SOC parameter we used in this section ($\gamma_D = 23.9 \text{ eV} \cdot \text{\AA}^3$) is larger than the value ($\gamma_D = 8.2 \text{ eV} \cdot \text{\AA}^3$) fitted from experimental data (see Appendix A). However, as the DP spin relaxation is more than two orders of magnitude larger than the BAP spin relaxation, the choice of the γ_D does not change the conclusion that the BAP mechanism is unimportant.
- ⁷¹ Further calculation indicates that the results from Eq. (27) deviate more from our calculation via the KSBs than small spin polarization as the Pauli blocking of spin-flip scattering is more pronounced when both spin bands are nearly equally populated.
- ⁷² According to Eq. (26), the effect of the Coulomb HF term can be estimated by $\tau_s(P) = \tau_s(P=0) [1 + (V_{q_0} n_e P \tau_p^*)^2]$ where V_{q_0} describes the average Coulomb interaction with q_0 , n_e , P being the average momentum, the electron density, and the initial spin polarization. Thus the effect of the Coulomb HF term is more pronounced for larger n_e , P and weaker scattering (i.e., larger τ_p^*). Moreover, increase of the temperature would reduce the effect as q_0 becomes larger and V_{q_0} becomes smaller.
- ⁷³ S. Oertel, J. Hübner, and M. Oestreich, Appl. Phys. Lett. **93**, 132112 (2008).
- ⁷⁴ The EY mechanism is checked to be unimportant in the parameter region we studied for both p -GaAs and p -GaSb.
- ⁷⁵ H. Haug and S. W. Koch, *Quantum Theory of the Optical and Electronic Properties of Semiconductors* (World Scientific, Singapore, 2004), 4th ed.
- ⁷⁶ J. H. Jiang, Y. Zhou, T. Korn, C. Schüller, and M. W. Wu, arXiv:0901.0061.
- ⁷⁷ J. Y. Fu and M. W. Wu, J. Appl. Phys. **104**, 093712 (2008).
- ⁷⁸ J. L. Cheng, Ph.D. Dissertation, University of Science and Technology of China, 2007.